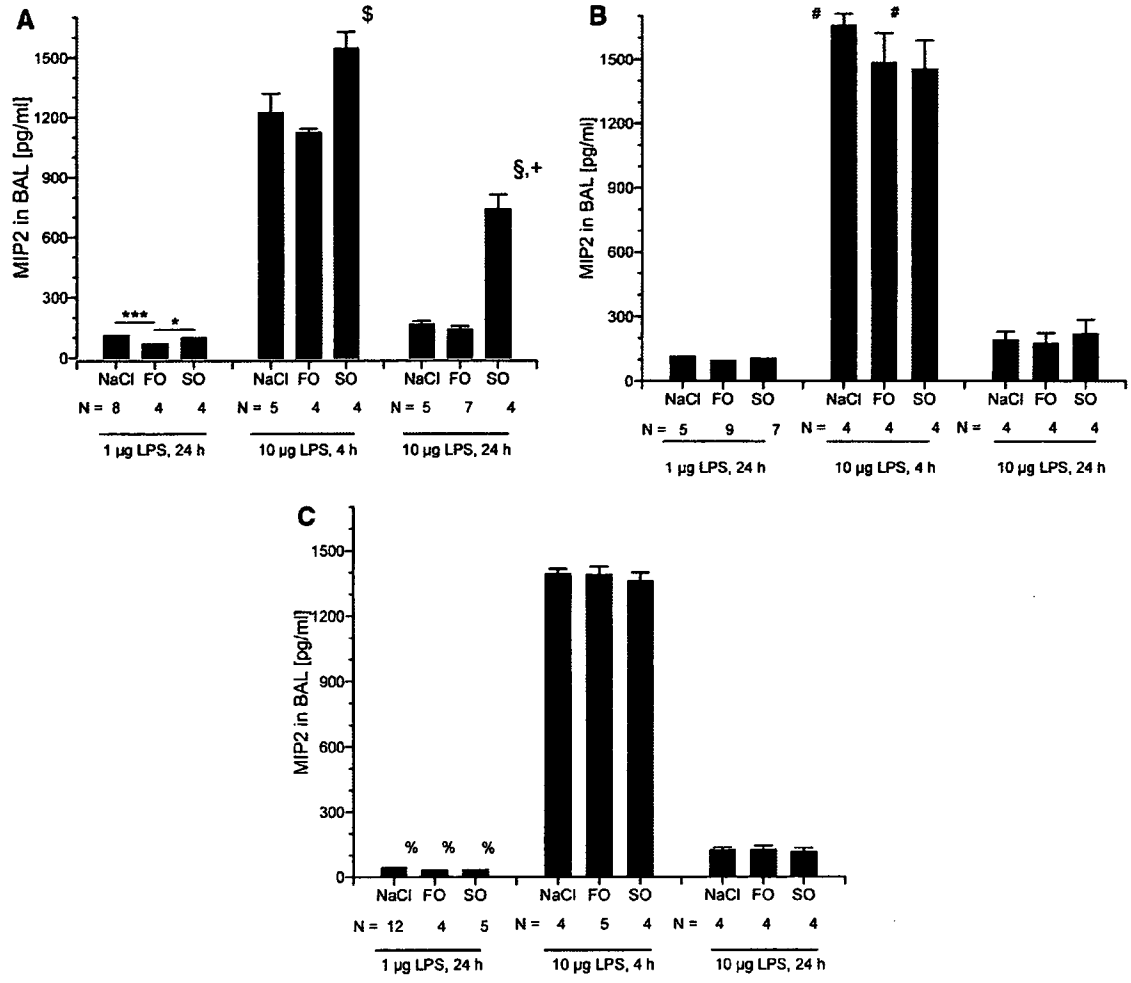

Figure 2. Impact of fish oil (*FO*)- vs. soybean oil (*SO*)-based lipid infusions on alveolar macrophage inflammatory protein (*MIP*)-2 generation in wild-type (WT) mice, mice lacking the platelet-activating factor-receptor (PAF-R −/−), and WT mice treated with platelet-activating factor receptor antagonist (PAF-RA) in a model of acute lung injury. WT mice (*A*), PAF-R −/− mice (*B*), and WT mice treated with a PAF-RA (*C*) were infused for 3 days with normal saline (control) or FO- or SO-based lipid emulsions, followed by stimulation with 1 or 10 µg of endotoxin (lipopolysaccharide, LPS) intratracheally 4 or 24 hrs before lavage. MIP-2 concentrations in bronchoalveolar lavage (*BAL*) were determined by enzyme-linked immunosorbent assay. Infusion of FO lipid emulsions resulted in decreased MIP-2 formation in WT mice (*$p < .05$ vs. SO; ***$p < .001$ vs. control). Infusion of SO resulted in increased MIP-2 generation compared with control and FO in both 10-µg groups ($\$p < .05$; $\S p < .001$). In PAF-R −/− or in WT mice treated with PAF-RA, no significant impact of lipid emulsions could be detected. MIP-2 concentrations in PAF-R −/− mice receiving 10 µg of LPS were higher after 4 hrs compared with corresponding WT controls ($\#p < .05$). After 24 hrs in WT-SO mice challenged with 10 µg of LPS, MIP-2 was significantly higher compared with the corresponding infusion groups of PAF-R −/− and PAF-RA mice ($+p < .01$). All infusion groups of PAF-RA mice receiving 1 µg of LPS were significantly lower than corresponding PAF-R −/− and WT groups ($\%p < .05$). Data are given as mean ± SEM. Numbers of animals per group are detailed below columns. Error bars are missing when falling into symbol.

(n = 5) without significant impact of the lipid emulsions. Two hours after intraperitoneal LPS challenge, 7.5 ± 0.8 × 10^9/L leukocytes were found in peripheral blood in mice receiving normal saline (n = 4). After FO infusion, leukocytes were slightly lower and SO slightly increased peripheral leukocytes; however, no significant difference was found.

Before LPS instillation in PAF-R −/− mice, leukocyte counts in peripheral blood were slightly higher compared with WT mice (7.2 ± 0.5 × 10^9/L, n = 4). Again, no significant impact of the lipid emulsions was found. After LPS injection into the peritoneal cavity, we detected 7.9 ± 1.6 × 10^9/L leukocytes in mice receiving NaCl. After FO or SO treatment, 8.5 ± 1.8 × 10^9/L and 7.1 ± 1.9 × 10^9/L leukocytes were measured (n = 4 each). However, no significant difference was found between infusion regimes.

Before LPS stimulation, no MIP-2 was detectable in plasma in either group. In WT controls, LPS challenge induced an increase to 9.0 ± 1.9 ng/mL. Infusion of FO-derived lipid emulsions resulted in a diminished MIP-2 serum concentration, whereas application of SO-based lipids increased MIP-2 levels significantly compared with the FO group ($p < .05$, Fig. 4*A*). In PAF-R −/−, LPS stimulation induced a three-fold increase in MIP-2 concentrations compared with WT in mice receiving NaCl ($p < .01$). This increase was also detected in both lipid infusion groups; however, differences between the infusion groups were abolished (Fig. 4*B*). The increase in MIP-2 was significant comparing PAF-R −/− mice with WT animals receiving FO ($p < .01$) but not in mice infused with SO.

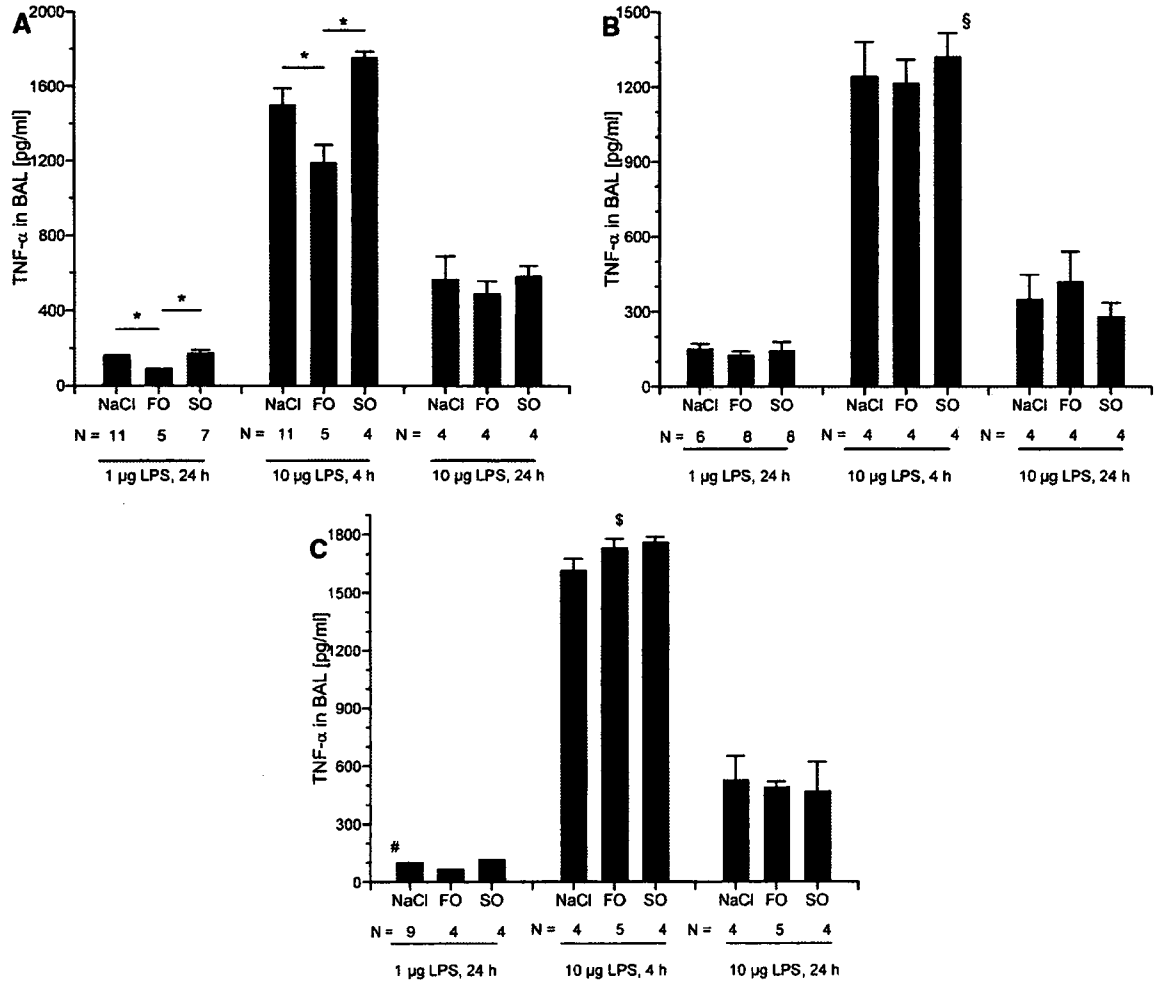

Figure 3. Impact of fish oil (*FO*)- vs. soybean oil (*SO*)-based lipid infusions on alveolar tumor necrosis factor (*TNF*)-α generation in wild-type (WT) mice, mice lacking the platelet-activating factor-receptor (PAF-R −/−), and WT mice treated with platelet-activating factor receptor antagonist (PAF-RA) in a model of acute lung injury. WT mice (*A*), PAF-R−/− mice (*B*), and WT mice treated with a PAF-RA (*C*) were infused for 3 days with saline (control) or FO- or SO-based lipid emulsions, followed by stimulation with 1 or 10 μg of endotoxin (lipopolysaccharide, LPS) intratracheally 4 or 24 hrs before lavage. TNF-α concentration in bronchoalveolar lavage was determined by enzyme-linked immunosorbent assay. Infusion of FO resulted in decreased TNF-α formation in WT mice (*$p < .05$ vs. SO and control). In PAF-R−/− mice or WT mice treated with PAF-RA, no significant impact of lipid emulsions could be detected. In PAF-RA mice challenged with 1 μg of LPS, TNF-α concentration of the NaCl group was lower compared with corresponding WT animals (#$p < .05$). After infusion of FO in PAF-RA mice, TNF-α concentration was higher compared with the WT-FO and PAF-R−/−-FO animals receiving 10 μg of LPS after 4 hrs ($$p < .05$). TNF-α concentration was lower in the PAF-R−/−-SO group after 10 μg of LPS and 4 hrs compared with the WT-SO and PAF-RA-SO animals (§$p < .05$). Data are given as mean ± SEM. Numbers of animals per group are detailed below columns. Error bars are missing when falling into symbol.

Before LPS challenge, we did not detect TNF-α in plasma in all groups. Following intraperitoneal LPS application, plasma TNF-α concentration rose to 303 ± 20 pg/mL in control animals. Infusion of SO-based lipids resulted in a significant increase of nearly 50% in TNF-α plasma concentration (Fig. 4*C*, $p < .01$ vs. control). After infusion of FO-derived lipids, TNF-α decreased significantly to 181 ± 12 pg/mL ($p < .05$ vs. control and $p < .001$ vs. SO). LPS challenge in PAF-R −/− mice infused with NaCl evoked a similar TNF-α concentration compared with WT controls (Fig. 4*D*). Again, no significant difference between the different infusion groups became detectable.

DISCUSSION

Using two different models of acute inflammation in mice, we have demonstrated that a 3-day course of lipid emulsion infusions is sufficient to modulate inflammatory responses induced by LPS. In contrast to SO-based lipid emulsions, FO-based lipid emulsions reduced pulmonary leukocyte invasion, protein leakage, and cytokine generation as well as cytokine appearance in the intravascular compartment. We present evidence that diverging effects of lipids emulsions are linked to PAF-R signaling. In mice carrying the disrupted PAF-R gene (PAF-R −/−), as well as in mice treated with a PAF-RA, the general response to endotoxin remained intact, but the differential response to FO vs. SO lipids was lost. A drawback of both models applied is the use of LPS in a single-hit model to induce inflammatory responses. Such a model is clearly different from clinical and experimental sepsis induced by bacterial infection.

Responses to endotoxin in PAF-R −/− mice were intact in our acute lung injury

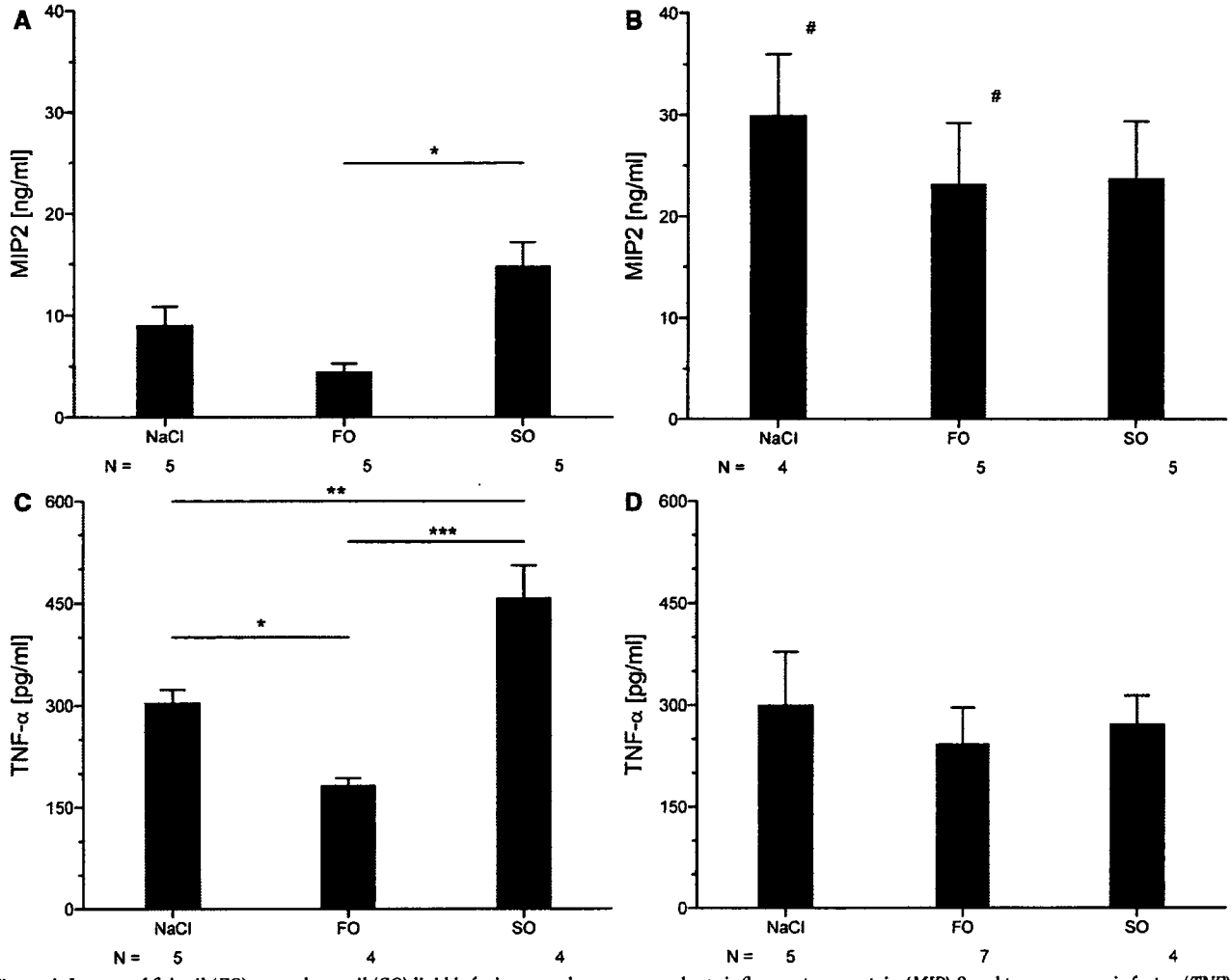

Figure 4. Impact of fish oil (*FO*) vs. soybean oil (*SO*) lipid infusions on plasma macrophage inflammatory protein (*MIP*)-2 and tumor necrosis factor (*TNF*)-α in wild-type (WT) mice and mice lacking the platelet-activating factor-receptor (PAF-R −/−) in a model of intraperitoneal inflammation. WT mice (*A*, *C*) or PAF-R−/− mice (*B*, *D*) were infused for 3 days with saline (control) or FO- or SO-based lipid emulsions, followed by stimulation with endotoxin (lipopolysaccharide, LPS) intraperitoneally 2 hrs before kill. MIP-2 (*A*, *B*) and TNF-α (*C*, *D*) in plasma were determined by enzyme-linked immunosorbent assay. Infusion of FO resulted in decreased MIP-2 formation in WT mice (*$p < .05$ vs. SO) but not in PAF-R−/− mice. TNF-α was increased after SO but decreased after FO compared with NaCl in WT mice receiving LPS (*$p < .05$; **$p < .01$; ***$p < .001$). MIP-2 was higher in PAF-R−/− mice after infusion with NaCl or FO compared with corresponding WT groups ($p < .01$). Data are given as mean ± SEM. Numbers of animals per group are detailed below columns.

model. These data are well in line with a previous report demonstrating regular responses of PAF-R −/− mice in an endotoxic shock model (15). Our data documenting elevated plasma levels of MIP-2 in PAF-R −/− mice compared with WT mice remain enigmatic. Elevated MIP-2 levels were observed both after lipid infusions and in saline controls. We speculate that this increase may be part of a long-term compensatory mechanism due to PAF-R deficiency, since PAF and MIP-2 may both act as chemoattractants. Further investigations are required to explain this phenomenon. In the PAF-RA group, the overall response to endotoxin remained intact. However, we found a delay in transmigration of leukocytes compared with WT mice: In mice receiving 10 μg of LPS, after 4 hrs leukocyte numbers were reduced but rose to an equal number of leukocytes after 24 hrs. Furthermore, we found a reduction of MIP2 and TNF-α in BAL in mice receiving 1 μg of LPS but not after 10 μg of endotoxin.

A striking finding of the present study was the differential impact of the FO vs. SO on cytokine generation provoked by endotoxin challenge in WT mice. In mice undergoing conventional SO-based lipid infusion, an augmentation of TNF-α and MIP-2 (the murine equivalent of interleukin-8) concentration in response to LPS challenge was observed irrespective of the model employed. In contrast, infusion of FO in WT mice resulted in reduced proinflammatory cytokine generation under all experimental conditions investigated. Although this is the first report of continuous lipid infusion in murine acute lung injury, our observations are consistent with previous findings demonstrating that TNF-α and interleukin-1 release was suppressed by dietary n-3 fatty acids in isolated murine splenocytes (25) and in isolated monocytes obtained from septic patients undergoing FO-based lipid infusions (18). Several days to weeks of oral FO supplementation are usually necessary to achieve such a change, whereas a

3-day infusion course sufficed to cause changes in cytokine synthesis in the present study and in patients receiving intravenous lipids (18). However using continuous enteral feeding, Gadek et al. (16) found a rapid increase in n-3 fatty acids in plasma phospholipids. We speculate that a key issue may be the continuous delivery of higher doses of FO to achieve fast changes. Preliminary data in our model suggest a rapid increase in n-3 fatty acids in plasma after infusion of FO and increase in n-6 polyunsaturated fatty acids in the SO group.

Pulmonary leukocyte recruitment was reduced in WT mice receiving FO-derived lipid emulsions. In contrast, SO-derived n-6 lipids increased leukocyte invasion and lung injury. We and others have described increased injury to lungs undergoing inflammatory stress due to n-6 lipids and, vice versa, an amelioration of damage by administration of n-3 lipids (26, 27). Mechanisms underlying this protective effect include, at least in part, the effect of FO on cytokine response described previously, generation of less potent lipid mediators as leukotriene B_5 instead of leukotriene B_4, formation of the less active vasoconstrictor thromboxane A_3 instead of thromboxane A_2, a reduction in platelet-activating factor synthesis, and reduced adhesion of leukocytes to endothelial cells (28–30). Transmigration of leukocytes through the endothelial-epithelial structures is a complex and tightly regulated process. The n-3 lipids interfere with this process at multiple stages, involving reduced presentation of endothelial adhesion molecules and reduced formation of platelet-activating factor by endothelial cells, which may then result in diminished activation of integrins on rolling leukocytes (28, 31). Furthermore, addition of arachidonic acid to endothelial cells increased thrombin-induced formation of PAF; in contrast, supplementation with n-3 fatty acids reduced its formation (28). As PAF generated by endothelial cells is not secreted to the supernatant but remains bound to the cell membrane, it may activate rolling leukocytes by binding to their PAF-R and initiate adhesion and transmigration (32). This mechanism may be at least in part responsible for the reduced rolling and adhesion of monocytes to endothelial cells after exposure to n-3 fatty acids and may translate in reduced transmigration of leukocytes (28).

Infusion of lipid emulsions bypasses physiologic uptake and processing of triglycerides by the gastrointestinal tract. Instead, infusion of synthetic lipid aggregates activates endothelial lipoprotein lipases, with translocation of the enzyme from its cellular binding sites into vascular compartment. Activation and translocation of this enzyme result in an increase in plasma free fatty acids due to avoidance of local cellular uptake mechanisms (33). The kinetics and duration of elevated plasma n-3 lipid levels thus exceed the corresponding alterations in response to conventional dietary FO uptake by orders of magnitude (34). Different availability of precursor fatty acids not only has an impact on subsequent generation of lipid mediators (e.g., substitution of leukotriene B_5 for B_4) but also reduces the generation of PAF due to incorporation into the phospholipid-precursor pool. In this respect, at least two lipid-dependent mechanisms may be relevant. First, enrichment of n-3 fatty acids in the PAF precursor pool may result in steric inhibition of phospholipase A_2 (32). Conversely, the increasing availability of arachidonic acid enhances generation of platelet-activating factor (28). Second, increasing n-3 fatty acids in phosphatidyl-inositol may impair the activation of leukocytes through reduction in intracellular second-messenger generation and activation of protein kinase C (7).

Recent experimental and clinical investigations suggest a strong link between the availability of free arachidonic acid, PAF, and lung injury. PAF and LPS promote lung injury and edema through sphingomyelinase-dependent formation of ceramide and activation of the cyclooxygenase pathway, which leads to the generation of arachidonic acid-derived prostanoids (35). Rapid infusion of conventional lipid emulsions in mechanically ventilated patients suffering from acute respiratory distress syndrome increased pulmonary shunt, notably linked to enhanced prostanoid generation resulting in a deterioration of the Pao_2/Fio_2 ratio (36). A second study in acute respiratory distress syndrome patients undergoing lipid infusions reported an increase in BAL PAF concentration and neutrophil counts paralleled by a deterioration in lung function, as measured by decreased Pao_2/Fio_2 (37). Despite these results and experimental use of PAF-RAs exhibiting beneficial properties in models of sepsis and acute lung injury (12, 38), phase III clinical studies using PAF-RAs or PAF-acetylhydrolase in septic patients have failed to show a difference in survival (13, 14). There may be a gap between experimental studies, when sepsis is initiated by a single LPS challenge with simultaneously started treatment, and clinical reality. Furthermore, as the response to LPS was intact in our model using PAF-R −/− mice, it remains to be determined if other inflammatory response systems may compensate for the inhibited PAF pathway.

However, the role of PAF in lipid infusion-related deterioration of lung function is underscored by our experiments using mice with a targeted disruption of the PAF receptor gene. Employing this strain, we were able to demonstrate that intratracheal LPS instillation provoked recruitment of leukocytes, as well as TNF-α and MIP-2 generation to the same extent as in WT mice, a phenomenon already described (15). Nevertheless, aggravation of lung inflammation by SO and its amelioration by FO-derived emulsions were essentially abolished in mice lacking this receptor. These results were confirmed in WT mice treated with a PAF-RA. Using BN52021, the differential impact of FO vs. SO on leukocyte recruitment and cytokine generation was also blocked. We conclude that major proinflammatory effects of conventional lipid emulsions and the ameliorating impact of FO-derived lipid emulsions on inflammation and pulmonary injury are linked to the integrity of PAF and PAF-R-related signaling in mice.

The correct timing and dosing of any pro- or anti-inflammatory drug in inflammation and sepsis are currently unsettled. N-3/n-6 ratios of 7.6:1 (FO) or 1:370 (safflower oil) have immune-suppressive features in a heart transplantation model (39), and application of SO (ratio 1:6.4) in septic patients increased the cytokine response (19). However, a ratio of 1:2 was shown to have only a minor impact on immunity in the heart transplantation model (39). Applying an n-3/n-6 ratio of 1:2 or 1:3 may therefore be a means to evade immune-modulating effects. Whereas FO in a hyperinflammatory state may be judged as an adjunct therapy, it may prove not to be beneficial in patients with already reduced immune response. Nevertheless, recent data from an observational study in 661 patients including 276 septic patients suggest that supplementation of parenteral nutrition with 0.1–0.2 g/kg/day FO had favorable effects on survival rate, infection rates, and length of stay in this subgroup (40). In addition, current studies using an enteral immune-modulating diet including n-3 fatty ac-

ids in patients with acute respiratory distress syndrome or sepsis show improvement in Pao_2/Fio_2 ratio, reduction in ventilation time, and even improvement in survival (16, 41, 42).

CONCLUSIONS

We demonstrated that infusion of FO-based lipid emulsions reduces LPS-induced proinflammatory cytokines, alveolar leukocyte transmigration, and protein leakage. In contrast, SO-based lipids lead to a further increase in the inflammatory response. However, the effect of lipid emulsions in murine inflammation is dependent on an intact PAF/PAF-R signaling. Administration of lipid emulsions not only may be regarded as a simple supply of calories but may also modulate the inflammatory response.

REFERENCES

1. Martin GS, Mannino DM, Eaton S, et al: The epidemiology of sepsis in the United States from 1979 through 2000. *N Engl J Med* 2003; 348:1546–1554
2. Brun-Buisson C, Minelli C, Bertolini G, et al: Epidemiology and outcome of acute lung injury in European intensive care units. Results from the ALIVE study. *Intensive Care Med* 2004; 30:51–61
3. Heller A, Koch T, Schmeck J, et al: Lipid mediators in inflammatory disorders. *Drugs* 1998; 55:487–496
4. Hotchkiss RS, Karl IE: The pathophysiology and treatment of sepsis. *N Engl J Med* 2003; 348:138–150
5. Mayer K, Schaefer MB, Seeger W: Fish oil in the critically ill: From experimental to clinical data. *Curr Opin Clin Nutr Metab Care* 2006; 9:140–148
6. Calder PC: Immunoregulatory and anti-inflammatory effects of n-3 polyunsaturated fatty acids. *Braz J Med Biol Res* 1998; 31: 467–490
7. Sperling RI, Benincaso AI, Knoell CT, et al: Dietary omega-3 polyunsaturated fatty acids inhibit phosphoinositide formation and chemotaxis in neutrophils. *J Clin Invest* 1993; 91:651–660
8. Denys A, Hichami A, Khan NA: n-3 PUFAs modulate T-cell activation via protein kinase C-alpha and -epsilon and the NF-kappaB signaling pathway. *J Lipid Res* 2005; 46: 752–758
9. Grimble RF, Howell WM, O'Reilly G, et al: The ability of fish oil to suppress tumor necrosis factor alpha production by peripheral blood mononuclear cells in healthy men is associated with polymorphisms in genes that influence tumor necrosis factor alpha production. *Am J Clin Nutr* 2002; 76:454–459
10. Zimmerman GA, McIntyre TM, Prescott SM, et al: The platelet-activating factor signaling system and its regulators in syndromes of inflammation and thrombosis. *Crit Care Med* 2002; 30:S294–S301
11. Leitinger N: Oxidized phospholipids as modulators of inflammation in atherosclerosis. *Curr Opin Lipidol* 2003; 14:421–430
12. Mathiak G, Szewczyk D, Abdullah F, et al: Platelet-activating factor (PAF) in experimental and clinical sepsis. *Shock* 1997; 7:391–404
13. Opal S, Laterre PF, Abraham E, et al: Recombinant human platelet-activating factor acetylhydrolase for treatment of severe sepsis: Results of a phase III, multicenter, randomized, double-blind, placebo-controlled, clinical trial. *Crit Care Med* 2004; 32: 332–341
14. Dhainaut JF, Tenaillon A, Hemmer M, et al: Confirmatory platelet-activating factor receptor antagonist trial in patients with severe gram-negative bacterial sepsis: A phase III, randomized, double-blind, placebo-controlled, multicenter trial. BN 52021 Sepsis Investigator Group. *Crit Care Med* 1998; 26: 1963–1971
15. Ishii S, Kuwaki T, Nagase T, et al: Impaired anaphylactic responses with intact sensitivity to endotoxin in mice lacking a platelet-activating factor receptor. *J Exp Med* 1998; 187:1779–1788
16. Gadek JE, DeMichele SJ, Karlstad MD, et al: Effect of enteral feeding with eicosapentaenoic acid, gamma-linolenic acid, and antioxidants in patients with acute respiratory distress syndrome. Enteral Nutrition in ARDS Study Group. *Crit Care Med* 1999; 27:1409–1420
17. Guarini P, Bellavite P, Biasi D, et al: Effects of dietary fish oil and soy phosphatidylcholine on neutrophil fatty acid composition, superoxide release, and adhesion. *Inflammation* 1998; 22:381–391
18. Mayer K, Gokorsch S, Fegbeutel C, et al: Parenteral nutrition with fish oil modulates cytokine response in patients with sepsis. *Am J Respir Crit Care Med* 2003; 167: 1321–1328
19. Mayer K, Meyer S, Reinholz-Muhly M, et al: Short-time infusion of fish oil-based lipid emulsions, approved for parenteral nutrition, reduces monocyte proinflammatory cytokine generation and adhesive interaction with endothelium in humans. *J Immunol* 2003; 171: 4837–4843
20. Maus UA, Koay MA, Delbeck T, et al: Role of resident alveolar macrophages in leukocyte traffic into the alveolar air space of intact mice. *Am J Physiol Lung Cell Mol Physiol* 2002; 282:L1245–L1252
21. Lowry OH, Rosebrough NJ, Farr AL, et al: Protein measurement with the Folin phenol reagent. *J Biol Chem* 1951; 193:265–275
22. Andonegui G, Bonder CS, Green F, et al: Endothelium-derived Toll-like receptor-4 is the key molecule in LPS-induced neutrophil sequestration into lungs. *J Clin Invest* 2003; 111:1011–1020
23. Parker JC, Townsley MI: Evaluation of lung injury in rats and mice. *Am J Physiol Lung Cell Mol Physiol* 2004; 286:L231–L246
24. Inoue K, Takano H, Shimada A, et al: Urinary trypsin inhibitor protects against systemic inflammation induced by lipopolysaccharide. *Mol Pharmacol* 2005; 67:673–680
25. Ishihara K, Komatsu W, Saito H, et al: Comparison of the effects of dietary alpha-linolenic, stearidonic, and eicosapentaenoic acids on production of inflammatory mediators in mice. *Lipids* 2002; 37:481–486
26. Grimminger F, Wahn H, Mayer K, et al: Impact of arachidonic versus eicosapentaenoic acid on exotonin-induced lung vascular leakage: Relation to 4-series versus 5-series leukotriene generation. *Am J Respir Crit Care Med* 1997; 155:513–519
27. Murray MJ, Kumar M, Gregory TJ, et al: Select dietary fatty acids attenuate cardiopulmonary dysfunction during acute lung injury in pigs. *Am J Physiol* 1995; 269: H2090–H2099
28. Mayer K, Merfels M, Muhly-Reinholz M, et al: Omega-3 fatty acids suppress monocyte adhesion to human endothelial cells: Role of endothelial PAF generation. *Am J Physiol Heart Circ Physiol* 2002; 283:H811–H818
29. Grimminger F, Mayer K, Kiss L, et al: PAF-induced synthesis of tetraenoic and pentaenoic leukotrienes in the isolated rabbit lung. *Am J Physiol Lung Cell Mol Physiol* 2000; 278:L268–L275
30. Murray MJ, Zhang T: The incorporation of dietary n-3 polyunsaturated fatty acids into porcine platelet phospholipids and their effects on platelet thromboxane A2 release. *Prostaglandins Leukot Essent Fatty Acids* 1997; 56:223–228
31. Weber C, Erl W, Pietsch A, et al: Docosahexaenoic acid selectively attenuates induction of vascular cell adhesion molecule-1 and subsequent monocytic cell adhesion to human endothelial cells stimulated by tumor necrosis factor-alpha. *Arterioscler Thromb Vasc Biol* 1995; 15:622–628
32. Prescott SM, Zimmerman GA, McIntyre TM: Platelet-activating factor. *J Biol Chem* 1990; 265:17381–17384
33. Peterson J, Bihain BE, Bengtsson-Olivecrona G, et al: Fatty acid control of lipoprotein lipase: A link between energy metabolism and lipid transport. *Proc Natl Acad Sci U S A* 1990; 87:909–913
34. Lovegrove JA, Brooks CN, Murphy MC, et al: Use of manufactured foods enriched with fish oils as a means of increasing long-chain n-3 polyunsaturated fatty acid intake. *Br J Nutr* 1997; 78:223–236
35. Goggel R, Winoto-Morbach S, Vielhaber G, et al: PAF-mediated pulmonary edema: A new role for acid sphingomyelinase and ceramide. *Nat Med* 2004; 10:155–160
36. Suchner U, Katz DP, Furst P, et al: Effects of intravenous fat emulsions on lung function in patients with acute respiratory distress syndrome or sepsis. *Crit Care Med* 2001; 29: 1569–1574

37. Lekka ME, Liokatis S, Nathanail C, et al: The impact of intravenous fat emulsion administration in acute lung injury. *Am J Respir Crit Care Med* 2004; 169:638–644
38. Christman BW, Lefferts PL, Blair IA, et al: Effect of platelet-activating factor receptor antagonism on endotoxin-induced lung dysfunction in awake sheep. *Am Rev Respir Dis* 1990; 142:1272–1278
39. Grimm H, Tibell A, Norrlind B, et al: Immunoregulation by parenteral lipids: Impact of the n-3 to n-6 fatty acid ratio. *JPEN J Parenter Enteral Nutr* 1994; 18:417–421
40. Heller AR, Rossler S, Litz RJ, et al: Omega-3 fatty acids improve the diagnosis-related clinical outcome. *Crit Care Med* 2006; 34:972–979
41. Singer P, Theilla M, Fisher H, et al: Benefit of an enteral diet enriched with eicosapentaenoic acid and gamma-linolenic acid in ventilated patients with acute lung injury. *Crit Care Med* 2006; 34:1033–1038
42. Pontes-Arruda A, Aragao AM, Albuquerque JD: Effects of enteral feeding with eicosapentaenoic acid, gamma-linolenic acid, and antioxidants in mechanically ventilated patients with severe sepsis and septic shock. *Crit Care Med* 2006; 34:2325–2333

THE JOURNAL OF BIOLOGICAL CHEMISTRY VOL. 282, NO. 8, pp. 5814–5824, February 23, 2007

LPA_4/p2y_9/GPR23 Mediates Rho-dependent Morphological Changes in a Rat Neuronal Cell Line*

Received for publication, June 21, 2006, and in revised form, December 15, 2006 Published, JBC Papers in Press, December 17, 2006, DOI 10.1074/jbc.M610767200

Keisuke Yanagida‡, Satoshi Ishii‡§1, Fumie Hamano‡, Kyoko Noguchi‡, and Takao Shimizu‡

From the ‡Department of Biochemistry and Molecular Biology, Faculty of Medicine, the University of Tokyo and the §Precursory Research for Embryonic Science and Technology (PRESTO) of Japan Science and Technology Agency, 7-3-1 Hongo, Bunkyo-ku, Tokyo 113-0033, Japan

Lysophosphatidic acid (LPA) is a potent lipid mediator that evokes a variety of biological responses in many cell types via its specific G protein-coupled receptors. In particular, LPA affects cell morphology, cell survival, and cell cycle progression in neuronal cells. Recently, we identified p2y_9/GPR23 as a novel fourth LPA receptor, LPA_4 (Noguchi, K., Ishii, S., and Shimizu, T. (2003) *J. Biol. Chem.* 278, 25600–25606). To assess the functions of LPA_4 in neuronal cells, we used rat neuroblastoma B103 cells that lack endogenous responses to LPA. In B103 cells stably expressing LPA_4, we observed $G_{q/11}$-dependent calcium mobilization, but LPA did not affect adenylyl cyclase activity. In LPA_4 transfectants, LPA induced dramatic morphological changes, *i.e.* neurite retraction, cell aggregation, and cadherin-dependent cell adhesion, which involved Rho-mediated signaling pathways. Thus, our results demonstrated that LPA_4 as well as LPA_1 couple to $G_{q/11}$ and $G_{12/13}$, whereas LPA_4 differs from LPA_1 in that it does not couple to $G_{i/o}$. Through neurite retraction and cell aggregation, LPA_4 may play a role in neuronal development such as neurogenesis and neuronal migration.

Lysophosphatidic acid (LPA,[2] 1- or 2-acyl-*sn*-glycero-3-phosphate) is a naturally occurring bioactive lipid mediator that controls growth, motility, and differentiation (1). LPA plays important roles in many biological processes, such as brain development, oncogenesis, wound healing, and immune functions (2). The effects of LPA on target cells are mediated by activation of its specific G protein-coupled receptors (GPCRs). The LPA_1 (3), LPA_2 (4), and LPA_3 (5) receptors are the major members of the endothelial differentiation gene (EDG) family that interact with LPA. Pharmacological studies suggest that both LPA_1 and LPA_2 couple to at least three types of G proteins, $G_{i/o}$, G_q, and $G_{12/13}$, whereas LPA_3 couples to $G_{i/o}$ and G_q but not $G_{12/13}$ (6). Depending on the functional coupling of a given LPA receptor to G proteins, LPA activates diverse signaling cascades involving phosphoinositide 3-kinase, phospholipase C, mitogen-activated protein kinase, Rho family GTPase, and adenylyl cyclase (2, 7).

LPA is present in the brain at relatively high levels compared with other organs (8, 9). LPA influences the cell morphology of several neuronal cell lines, neural progenitors, and primary neurons (10). It has also been reported that LPA affects electrophysiology, cell survival, and cell cycle progression in neuronal cells (10, 11). Targeted deletion of LPA_1 in mice produces olfactory deficits (12) and a behavioral abnormality (13). Furthermore, the use of LPA_1 knockouts revealed that LPA_1 is involved in the initiation of neuropathic pain (14). Exposure of the developing cerebral cortex to LPA produces dramatic changes in the folding of the brain, which do not occur in LPA_1 and LPA_2 double knockouts (15). However, the LPA receptor subtypes responsible for some neuronal effects have not been identified (16–18).

Recently, we identified p2y_9/GPR23 as a fourth LPA receptor (LPA_4) that is structurally distinct from the three LPA receptors of the EDG family (19). The expressed sequence tag cDNA encoding LPA_4 was originally isolated from human brain (20, 21), and LPA_4 expression has been detected in rat embryonic hippocampal neurons (22) and immortalized hippocampal progenitor cells (18). These facts suggest that LPA_4 may have important roles in neurodevelopmental processes such as neurogenesis and neuronal migration. However, only very limited information is available regarding its physiological and biological functions. To assess the functional roles of LPA_4 in neuronal cells, we generated B103 cells stably expressing LPA_4. This study demonstrates that treatment of the LPA_4-expressing cells with LPA leads to morphological changes, including cell rounding and cadherin-dependent cell adhesion following cell aggregation, both of which are mediated by the Rho/Rho-associated kinase (ROCK) pathway. The effects of LPA_4 on the morphology of the neuronal cells were clearly distinct from those of LPA_1, probably because LPA_4 does not couple to $G_{i/o}$.

EXPERIMENTAL PROCEDURES

Cell Culture—B103 rat neuroblastoma cells were kindly provided by Dr. J. Chun (The Scripps Research Institute, La Jolla, CA). B103 cells expressing each of the LPA receptors were maintained on poly-L-lysine-coated 100-mm dishes (Iwaki,

* This work was supported by grants-in-aid from the Ministry of Education, Culture, Sports, Science, and Technology of Japan (to T. S. and S. I.). The costs of publication of this article were defrayed in part by the payment of page charges. This article must therefore be hereby marked "*advertisement*" in accordance with 18 U.S.C. Section 1734 solely to indicate this fact.

[1] To whom correspondence should be addressed: Dept. of Biochemistry and Molecular Biology, Faculty of Medicine, The University of Tokyo, 7-3-1 Hongo, Bunkyo-ku, Tokyo 113-0033, Japan. Tel.: 81-3-5802-2925; Fax: 81-3-3813-8732; E-mail: mame@m.u-tokyo.ac.jp.

[2] The abbreviations used are: LPA, lysophosphatidic acid; GPCR, G protein-coupled receptor; EDG, endothelial differentiation gene; ROCK, Rho-associated kinase; DMEM, Dulbecco's modified Eagle's medium; PTX, pertussis toxin; HA, hemagglutinin; PBS, phosphate-buffered saline; BSA, bovine serum albumin; HBSS, Hank's balanced salt solution; IBMX, 2-isobutyl-1-methylxanthine; $[Ca^{2+}]_i$, intracellular Ca^{2+} concentration; EGFP, enhanced green fluorescence proteins; S1P, sphingosine 1-phosphate; MEMF, mouse embryonic meningeal fibroblast; MSF, mouse skin fibroblast.

Tokyo, Japan) in Dulbecco's modified Eagle's medium (DMEM) (Sigma) supplemented with 10% fetal bovine serum (BioWhittaker, Walkersville, MD) and 0.3 mg/ml G418 (Wako, Osaka, Japan). For some experiments, cells were pretreated with 100 ng/ml pertussis toxin (PTX) (List Biological Laboratories, Campbell, CA; from a 400 μg/ml stock in 10 mM Tris-HCl (pH 7.4) and 2 M urea stored at 4 °C) for 12 h, 5 μM YM-254890 (a novel $G_{q/11}$ inhibitor (23), a kind gift from Dr. J. Takasaki, Astellas Pharma Inc., Tokyo, Japan; from a 10 mM stock in dimethyl sulfoxide (Sigma) stored at −30 °C) for 10 min, or 5 μM Y-27632 (Calbiochem; from a 5 mM stock in water stored at −30 °C) for 10 min. Pretreatment with vehicles of PTX and YM-254890 was used as a control.

Stable Expression of LPA_1 and LPA_4—A DNA fragment containing the entire open reading frame of LPA_1 (NCBI accession number NM_001401) was first amplified from a cDNA prepared from human brain poly(A)$^+$ RNA (Clontech) by PCR using *Pfu* turbo DNA polymerase (Stratagene, La Jolla, CA) and oligonucleotides (sense primer, 5′-AAGAAAATTTGTCTCCCGTAGCTCT-3′ and antisense primer, 5′-CATGAGTTGACTTTTCTCCTCTCTC-3′). The entire open reading frame of LPA_1 with an additional sequence encoding a hemagglutinin (HA) epitope (YPYDVPDYA) at the 5′-end was subsequently amplified from the resultant PCR products using KOD-Plus DNA polymerase (Toyobo, Osaka, Japan) and oligonucleotides (sense primer containing the KpnI and HA tag sequences, 5′-GGGGTACCGCCATGTACCCCTACGACGTGCCCGACTACGCCGCTGCCATCTCTACTTCC-3′ and antisense primer containing the SpeI sequence, 5′-GGACTAGTCTAAACCACAGAGTGGTCATT-3′). The resultant DNA fragment was digested with KpnI and SpeI and subsequently cloned into the mammalian expression vector pCXN2.1, a slightly modified version of pCXN2 (24) with multiple cloning sites, between the KpnI and SpeI sites. HA-tagged human LPA_4 cDNA was constructed and cloned into pCXN2.1 as described previously (19). B103 cells were transfected using the Lipofectamine 2000 reagent (Invitrogen). After 48 h, the transient expression of the HA epitope on the cell surface was confirmed by flow cytometric analysis (EPICS XL, Beckman Coulter, Fullerton, CA) with the 3F10 rat monoclonal anti-HA antibody (Roche Applied Science) and phycoerythrin-labeled anti-rat IgG (Beckman Coulter) as the secondary antibody. Stable transfectants were selected with 1 mg/ml G418 for 26 days. After staining the drug-resistant cells as described above, a group of HA-positive cells was sorted by flow cytometry (EPICS ALTRA, Beckman Coulter) and maintained with 0.3 mg/ml G418. Three weeks later, a second round of sorting was performed; the twice-immunopurified cells were used for experiments (termed B103-LPA_1 and B103-LPA_4 cells).

Binding Assay—Binding assay was done essentially as described previously (19), with minor modifications. Cells (4×10^6) were seeded in collagen-coated 100-mm plates (Iwaki), followed by 24 h of serum starvation. The cells were washed with phosphate-buffered saline (PBS) twice and scraped off. After further washing with binding buffer (25 mM HEPES-NaOH (pH 7.4), 10 mM $MgCl_2$, and 0.25 M sucrose), the cells were suspended in the buffer with additional protease inhibitor mixture (Complete, Roche Applied Science), sonicated three times at 15 watts for 30 s, and centrifuged at 800 × *g* for 10 min at 4 °C. The supernatant was further centrifuged at $10^5 \times g$ for 60 min at 4 °C, and resultant pellet was homogenized in ice-cold binding buffer. Binding assays were performed in 96-well plates in triplicate. 20 μg each of the membrane fractions from the twice-immunopurified cells was incubated in binding buffer containing 0.25% bovine serum albumin (BSA) (fatty acid-free, very low endotoxin grade; Serologicals Proteins, Kankakee, IL) with 2-fold serial dilutions (50–3.125 nM) of [^{3}H]LPA (1-oleoyl[*oleoyl*-9,10-^{3}H]LPA, 57 Ci/mmol; PerkinElmer Life Sciences) for 60 min at 4 °C. The bound [^{3}H]LPA was collected onto a Unifilter-96-GF/C (PerkinElmer Life Sciences) using a MicroMate 196 harvester (Packard Instrument Co.). The filter was then rinsed 10 times with ice-cold binding buffer and dried for 12 h at 50 °C. 25 μl of MicroScint-0 scintillation mixture (PerkinElmer Life Sciences) was added per well. The radioactivity that remained on the filter was measured with TopCount microplate scintillation counter (Packard Instrument Co.). Total and nonspecific bindings were evaluated in the absence and presence of 10 μM unlabeled LPA [1-*oleoyl* (18:1)-LPA; Cayman Chemical, Ann Arbor, MI), respectively. The specific binding value (disintegrations/min) was calculated by subtracting the nonspecific binding value (disintegrations/min) from the total binding value (disintegrations/min). A dissociation constant (K_d) and a maximum binding capacity (B_{max}) were calculated by Scatchard analysis. B_{max} and K_d values for B103-LPA_1 cells were 0.8 pmol/mg protein and 18 nM, respectively. Those for B103-LPA_4 cells were 6.0 pmol/mg protein and 58 nM. No specific binding was observed in vector-transfected B103 cells (B103-vector cells).

cAMP Measurement—Cells (3.2×10^4) were seeded in collagen-coated 96-well plates (Iwaki), followed by 24 h of serum starvation. To determine whether LPA receptors mediate the inhibition of adenylyl cyclase, an AlphaScreen cAMP assay kit (PerkinElmer Life Sciences) was used as recommended in the manufacturer's instructions. The cells were washed twice with buffer A (Hanks' balanced salt solution (HBSS) containing 25 mM HEPES-NaOH (pH 7.4) and 0.1% BSA (Serologicals Proteins)) and incubated in 100 μl of buffer A containing 0.5 mM 3-isobutyl-1-methylxanthine (IBMX))(from a 20 mM stock in dimethyl sulfoxide stored at −30 °C) (Sigma) for 15 min at room temperature. The reaction was initiated by adding 50 μl of various concentrations of LPA in buffer A with 50 μM forskolin (Wako; from a 10 mM stock in dimethyl sulfoxide stored at −30 °C). After 30 min of incubation at room temperature, the reaction was terminated by adding 16.6 μl of 10% Tween 20, followed by overnight storage at 4 °C. After centrifugation at 800 × *g* for 5 min, the cAMP concentration in the supernatant was measured in quadruplicate with a fusion system (PerkinElmer Life Sciences). To determine whether LPA receptors mediate the stimulation of adenylyl cyclase, the cAMP Biotrak EIA system (Amersham Biosciences) was used as recommended in the manufacturer's instructions. The cells were washed twice with HEPES-Tyrode's buffer (25 mM HEPES-NaOH (pH 7.4), 140 mM NaCl, 2.7 mM KCl, 1 mM $CaCl_2$, 0.49 mM $MgCl_2$, 12 mM $NaHCO_3$, 0.37 mM NaH_2PO_4, and 5.6 mM D-glucose) containing 0.1% BSA (HEPES-Tyrode's BSA buffer) and incubated in 100 μl of HEPES-Tyrode's BSA buffer con-

taining 0.5 mM IBMX for 15 min at 37 °C. The reaction was initiated by adding 100 μl of various concentrations of LPA in HEPES-Tyrode's BSA buffer. After 30 min of incubation at 37 °C, the reaction was terminated by adding 25 μl of lysis buffer. Cell lysates in a volume of 100 μl were used to determine the cAMP concentration using an enzyme immunoassay method.

Ca^{2+} Measurement—Cells serum-starved for 24 h were detached with PBS containing 2 mM EDTA, washed with HEPES-Tyrode's buffer, and then loaded with 3 μM Fura-2 AM (Dojindo, Kumamoto, Japan) in HEPES-Tyrode's BSA buffer for 1 h at 37 °C. The cells were washed twice and resuspended in HEPES-Tyrode's BSA buffer at a density of 1×10^6 cells/ml. The cell suspension (0.5 ml) was applied to a CAF-100 spectrofluorometer (Jasco, Tokyo, Japan), and 5 μl of 100 μM LPA in HEPES-Tyrode's BSA buffer was added. The intracellular Ca^{2+} concentration ($[Ca^{2+}]_i$) was measured as the ratio of emission fluorescence at 500 nm in response to excitation at 340 and 380 nm.

Cell Rounding Assay—Cells (1×10^4) were seeded in poly-D-lysine-coated 12-well plates (BD Biosciences). After 24 h of incubation, the cells were washed three times with DMEM containing 0.1% BSA and serum-starved for 24 h. Three hours after a medium change, the cells were treated with 1 μM LPA for 15 min. The cells were examined for a round cell morphology lacking any neurite extensions or filopodia. Extended neurites were defined as having a length greater than the cell body. The number of rounded cells was expressed as a percentage of the observed cells (>200 cells/well).

Rho Inhibition Study—Cells (5×10^5) were seeded in poly-L-lysine-coated 35-mm dishes (Iwaki) in DMEM supplemented with 10% fetal bovine serum. After 24 h, either the *Clostridium botulinum* C3 exoenzyme expression vector (pEF-C3) (25) (a kind gift from Dr. S. Narumiya, Kyoto University, Kyoto, Japan) or the corresponding control vector (pEF-BOS) (26) (a kind gift from Dr. S. Nagata, Osaka University, Osaka, Japan) was cotransfected with an enhanced green fluorescent protein (EGFP) expression vector (pEGFP-C1; Clontech) at a 4:1 weight ratio, with 3 μg of total DNA, using the Lipofectamine 2000 reagent (Invitrogen). After 24 h, the cells were seeded in poly-D-lysine-coated 12-well plates and cultured for 24 h. The cells were then serum-starved for 12 h and treated with 1 μM LPA for 15 min. Following fixation with 1% paraformaldehyde for 15 min at 4 °C, EGFP images were obtained using a fluorescence microscope (Diaphoto, Nikon, Tokyo, Japan). EGFP-positive cells were examined for a round morphology without any neurite extensions or filopodia. At least 20 different fields were observed with a minimum of 100 EGFP-positive cells. The number of rounded cells was expressed as a percentage of the EGFP-positive cells.

Quantification of Cell Clustering—The degree of cell clustering was quantified by observing the distribution of the cell nuclei. Cells (1.5×10^5) were seeded in poly-D-lysine-coated 24-well plates (BD Biosciences). After 24 h of incubation, the cells were washed three times with DMEM containing 0.1% BSA and serum-starved for 24 h. Three hours after a medium change, the cells were treated with 1 μM LPA for 3 h, followed by fixation and staining with a Diff-Quik kit (Kokusai Shiyaku, Kobe, Japan). The distribution of the cells was mapped in rectangular areas (1710×1290 μm) by photographing the cultures (Cool Pix 990, Nikon). Each map was overlaid with grids at equal intervals (30 μm) and divided into 2451 unit squares. The randomness in spatial distribution was tested by counting the number of unit squares containing at least one nucleus. The intensity of the cell clustering was expressed as the percentage of the unit squares without any nuclei.

Cell Dissociation Assay—The Ca^{2+} sensitivity of cell-cell adhesion was estimated using trypsin treatment in the presence of either $CaCl_2$ (TC treatment) or EDTA (TE treatment) as described (27, 28), with minor modifications. Briefly, 5×10^5 cells were seeded in poly-D-lysine-coated 35-mm dishes (BD Biosciences) and cultured overnight. After 24 h of serum starvation, the cells were stimulated with 1 μM LPA for 2 h and washed with HBSS containing either 2 mM $CaCl_2$ or 2 mM EDTA. The washed cells were treated with 0.01% trypsin for 30 min at 37 °C and then dissociated by pipetting 10 times gently in 1 ml of HBSS with 0.01% trypsin. The number of cell clusters was counted with a particle counter (Beckman Coulter). The degree of cell-cell adhesion was expressed as the ratio of particles in the TC condition to particles in the TE condition (TC/TE). Negative control experiments without LPA treatment were also performed.

Western Blotting—Cells (4×10^6) were seeded in poly-L-lysine-coated 100-mm dishes. Following 24 h of serum starvation, the cells were treated with 1 μM LPA for 3 h, washed twice with PBS, and harvested in buffer B (25 mM HEPES-NaOH (pH 7.4), 10 mM $MgCl_2$, and 0.25 M sucrose). The cells were centrifuged at $800 \times g$ for 10 min at 4 °C, suspended in ice-cold buffer B containing 20 μM 4-amidinophenylmethylsulfonyl fluoride (Sigma) and a protease inhibitor mixture (Complete, Roche Applied Science), and sonicated three times for 30 s each at 4 °C. The cell debris was removed by centrifugation at $800 \times g$ for 10 min at 4 °C. The protein concentration of the homogenate was determined with a Bradford assay (Bio-Rad) using BSA as a standard. Five micrograms of protein sample containing 5% 2-mercaptoethanol was analyzed by 7.5% SDS-PAGE followed by transfer to a polyvinylidene difluoride membrane (Millipore Corp., Bedford, MA). The membrane was blocked with 5% skim milk (Difco) and probed with a mouse monoclonal antibody against N-cadherin or E-cadherin (BD Biosciences). The bands were visualized with an ECL chemiluminescence detection system (Amersham Biosciences) using horseradish peroxidase-conjugated anti-mouse IgG (Amersham Biosciences).

Immunofluorescence—Cells (3×10^5) were seeded into poly-L-lysine-coated glass-bottomed 35-mm dishes (Matsunami, Tokyo, Japan) and serum-starved for 24 h. Following stimulation with 1 μM LPA for 3 h at 37 °C, the cells were fixed with 4% paraformaldehyde for 20 min at 4 °C and rinsed twice with ice-cold PBS. Subsequently, the cells were incubated with a mouse monoclonal antibody against N-cadherin in PBS containing 1/4× permeabilization reagent (Beckman Coulter) for 1 h at room temperature. The primary antibody staining was visualized with an Alexa 488-conjugated goat anti-mouse IgG (Invitrogen). Images were obtained using an LSM510 laser-scanning confocal microscope (Carl Zeiss, Jena, Germany) equipped with an argon laser as the light source.

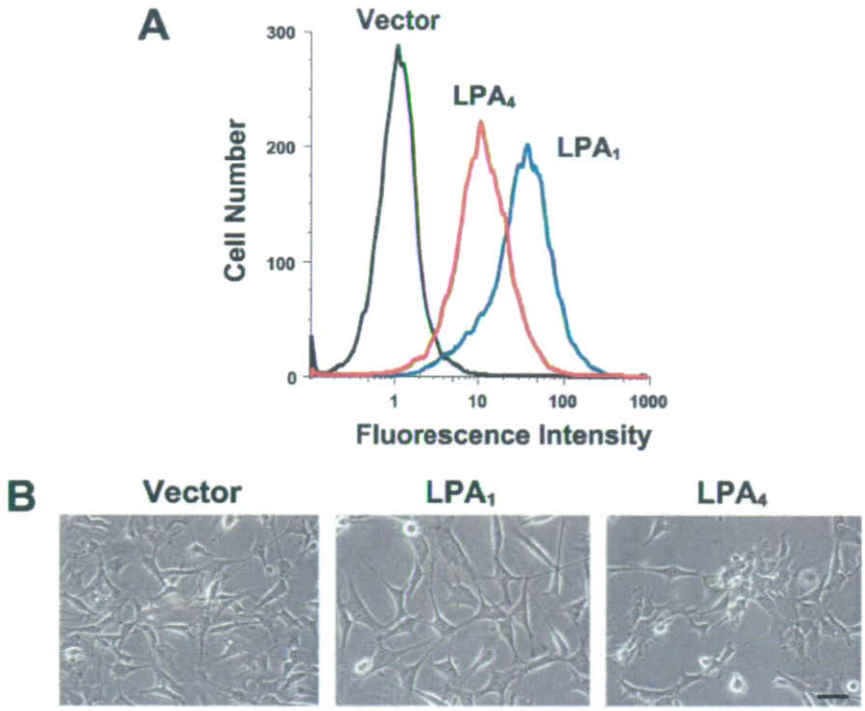

FIGURE 1. **Stable expression of LPA_1 or LPA_4 in B103 cells results in distinct morphologies.** *A*, flow cytometry analysis. B103 cells were stably transfected with the expression vectors for LPA_1 or LPA_4, each tagged with an HA epitope at the N terminus. After staining with an anti-HA antibody and a phycoerythrin-conjugated secondary antibody, HA-positive cells were sorted with a cell sorter and then subcultured. Data shown are the surface expression levels of the HA epitope in subcultured polyclonal cells obtained by the second round of cell sorting. Empty vector-transfected polyclonal cells served as a negative control. *B*, morphology of B103-vector, B103-LPA_1, and B103-LPA_4 cells in serum-containing medium. The cells were photographed 24 h after seeding. Each stable cell line showed similar growth rate. *Bar*, 40 μm.

Statistical Analysis—All values in the figures are expressed as means ± S.E. To determine statistical significance, the values were compared by analysis of variance followed by Tukey-Kramer test using Prism 4 software (GraphPad Software, San Diego, CA). The differences were considered significant if p values were less than 0.05.

RESULTS

Stable Expression of LPA_1 and LPA_4 in B103 Cells Results in Different Morphologies in Serum-containing Medium—To address the functional roles of LPA_4 in neuronal cells, B103 rat neuroblastoma cells were stably transfected with the expression vector for either LPA_1 or LPA_4. B103 cells were selected because they lack endogenous responses to LPA (29, 30). Consistently, no specific binding was observed in B103-vector cells in the radioligand binding assays (see "Experimental Procedures"). To determine the intrinsic gene expression profiles of LPA receptors in B103 cells, we performed a reverse transcription-PCR analysis of total cellular RNA from the cells. Although LPA_4 mRNA expression was slightly detected, no mRNA expression of the other three receptors, LPA_1, LPA_2, and LPA_3, was observed (data not shown). This finding is consistent with a recent report by Tsukahara *et al.* (31). The apparent discrepancy between the expression of LPA_4 and the lack of response to LPA might occur because the expression of LPA_4 is too low to respond to LPA. Alternatively, post-transcriptional/translational modifications (32) may produce discordance between mRNA and protein expression. Thus, we discounted the low expression of LPA_4 in B103 cells and took advantage of their unresponsiveness to LPA and their neuronal nature for the purpose of examining the functional roles of LPA_4 in neuronal cells.

For the construction of stably transfected cell lines, LPA_1 and LPA_4 were tagged with an HA epitope at the N terminus to enable us to determine the levels of expression on the cell surfaces. Fluorescence-activated cell sorting enriched a polyclonal population of the drug-resistant cells that expressed each LPA receptor. These populations of stable clones are free of any clonal deviation that could cause functional variations. Following two rounds of cell sorting, we observed that the fluorescence intensity of B103-LPA_1 cells was higher than that of B103-LPA_4 cells (Fig. 1*A*), although the B_{max} value for B103-LPA_1 cells (0.8 pmol/mg of protein) was lower than that for B103-LPA_4 cells (6.0 pmol/mg of protein). The apparent discrepancy might be because of two possibilities as follows: the usage of organellar membrane-rich microsome fractions and the difference in HA antibody immunoreactivity to the HA epitope tagged to two receptors. To confirm that no expression of the other subtypes of LPA receptors was enhanced secondary to the transfection, reverse transcription-PCR was performed with specific primers for LPA_1, LPA_2, LPA_3, and LPA_4 in B103-vector, B103-LPA_1, and B103-LPA_4 cells. As in the parental B103 cells, we observed only a low expression of LPA_4 and virtually no expression of the other LPA receptors in all of the transfected cell lines (data not shown).

Although these stably transfected cell lines showed similar growth rates (data not shown), they showed distinctly different morphologies in serum-containing medium (Fig. 1*B*). As reported previously (33), B103-LPA_1 cells displayed a flattened and more migratory morphology compared with B103-vector cells. Interestingly, B103-LPA_4 cells had an epithelial like morphology and appeared to adhere more tightly to each other than B103-vector cells. These observations suggest that LPA_1 and LPA_4 have distinct signaling pathways that produce different cell morphologies.

LPA_4 Does Not Affect Adenylyl Cyclase Activity in B103 Cells—We examined whether LPA_4 mediates the inhibition of adenylyl cyclase activity in B103 cells, as the other three LPA receptors do (30) (Fig. 2*A*). In B103-LPA_1 cells, LPA caused a dose-dependent inhibition of adenylyl cyclase activity with IC_{50} values below 10 nM (Fig. 2*A*). This inhibition was completely

blocked by PTX treatment, indicating the primary role of $G_{i/o}$ proteins. However, LPA at concentrations up to 10 μM did not blunt the forskolin-driven rises in cAMP accumulation in either B103-vector or B103-LPA$_4$ cells, suggesting that LPA$_4$ does not couple to $G_{i/o}$ proteins.

Previously, we reported that LPA induces cAMP accumulation in LPA$_4$-expressing Chinese hamster ovary cells (19). However, LPA did not elevate basal cAMP levels in either B103-LPA$_4$ cells or B103-LPA$_1$ cells (Fig. 2*B*), suggesting that neither LPA$_1$ nor LPA$_4$ couples to G_s in B103 cells.

LPA$_1$ and LPA$_4$ Mediate Ca^{2+} Mobilization via Distinct Signaling Pathways—LPA has been shown to induce intracellular Ca^{2+} mobilization in many cell types (34), and all EDG family LPA receptor subtypes mediate Ca^{2+} mobilization when expressed in B103 cells (30). We therefore examined whether LPA$_4$ mediates Ca^{2+} mobilization in B103 cells. Although B103-vector cells displayed no response to 1 μM LPA, increases in $[Ca^{2+}]_i$ were observed both in B103-LPA$_1$ and B103-LPA$_4$ cells (Fig. 3). LPA induces phospholipase C-mediated Ca^{2+} mobilization via the PTX-sensitive $G_{i/o}$- and/or PTX-insensitive $G_{q/11}$-mediated pathways (34). To examine the signaling pathways leading to Ca^{2+} mobilization in B103-LPA$_1$ and B103-LPA$_4$ cells, we treated the cells with a $G_{q/11}$-selective inhibitor, YM-254890 (23) (Fig. 3). ATP was used as a positive control, because ATP evokes Ca^{2+} mobilization via P2Y receptors predominantly through $G_{q/11}$ (35). The LPA-induced Ca^{2+} response in B103-LPA$_4$ cells and the ATP-induced Ca^{2+} response in both transfected cell lines were completely abolished by pretreatment with 5 μM YM-254890 (Fig. 3). In B103-LPA$_1$ cells, YM-254890 only partially inhibited the LPA-induced response (Fig. 3), but the combination of PTX and YM-254890 produced complete inhibition (data not shown). The degree of inhibition with YM-254890 in B103-LPA$_1$ cells was not altered at higher concentrations (up to 20 μM; data not shown), indicating that 5 μM YM-254890 was sufficient to inhibit the activation of $G_{q/11}$ proteins. These results suggest that both $G_{i/o}$ and $G_{q/11}$ proteins mediate Ca^{2+} mobilization in B103-LPA$_1$ cells, whereas $G_{q/11}$ is the dominant mediator of the response in B103-LPA$_4$ cells.

Both LPA$_1$ and LPA$_4$ Mediate Cell Rounding via Rho-dependent and $G_{i/o}$- and $G_{q/11}$-independent Pathways—LPA induces rapid growth cone collapse, neurite retraction, and neuronal cell rounding in several neuronal cell types

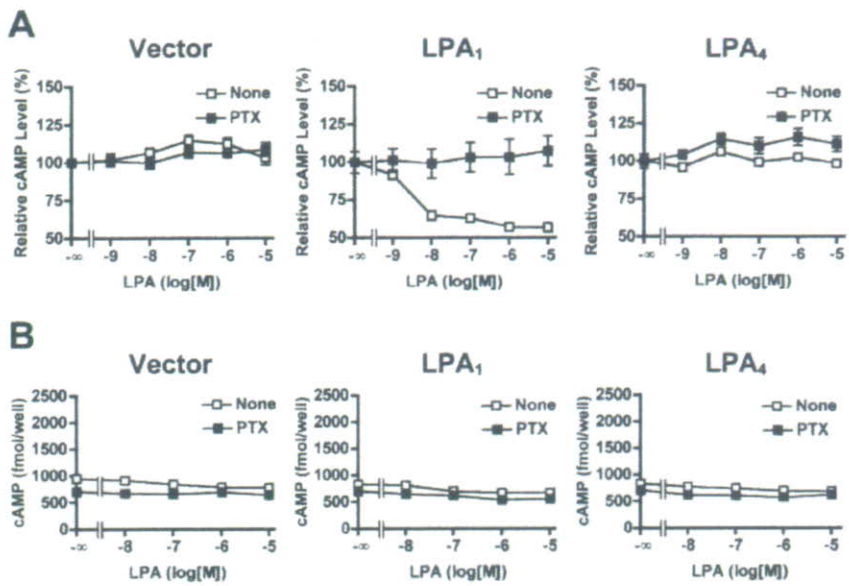

FIGURE 2. **LPA does not affect adenylyl cyclase activity in B103-LPA$_4$ cells.** *A*, failure of LPA to inhibit forskolin-induced cAMP accumulation in B103-LPA$_4$ cells. Serum-starved B103-vector, B103-LPA$_1$, and B103-LPA$_4$ cells were stimulated with increasing concentrations of LPA in the presence of 0.5 mM IBMX and 50 μM forskolin. After a 30-min incubation at room temperature, the cells were solubilized, and cAMP concentrations in the cell lysates were measured. Forskolin-induced cAMP accumulation in the absence of LPA was set to 100%. Where indicated, the cells were pretreated with 100 ng/ml PTX for 24 h. Data are means ± S.E. (n = 4) of a representative of three independent experiments with similar results. *B*, failure of LPA to induce cAMP accumulation in B103-LPA$_4$ cells. Serum-starved B103-vector, B103-LPA$_1$, and B103-LPA$_4$ cells were stimulated with increasing concentrations of LPA in the presence of 0.5 mM IBMX. After a 30-min incubation at room temperature, the cells were solubilized, and cAMP concentrations in the cell lysates were measured. The cells were pretreated with 100 ng/ml PTX for 24 h. Data are representative of three independent experiments with similar results.

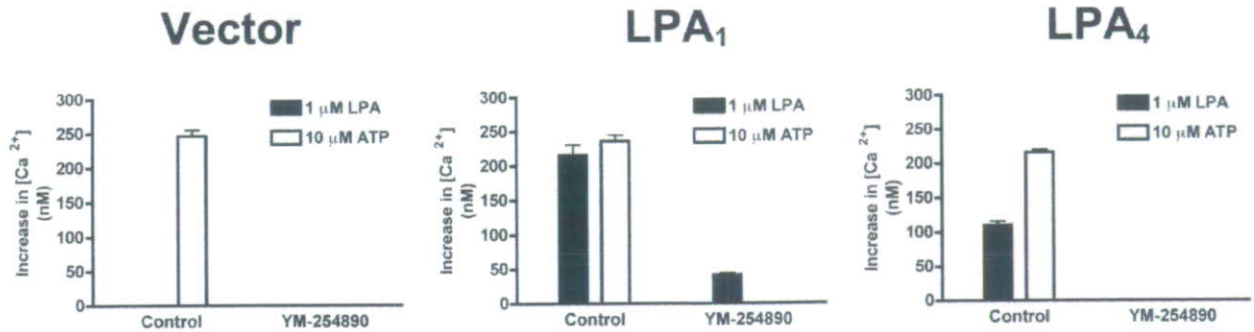

FIGURE 3. **LPA$_4$-mediated Ca^{2+} mobilization is entirely dependent on $G_{q/11}$ proteins.** B103-vector, B103-LPA$_1$, and B103-LPA$_4$ cells were serum-starved, loaded with 3 μM Fura-2 AM, and stimulated with 1 μM LPA or 10 μM ATP. Where indicated, the cells were pretreated with 5 μM YM-254890 for 10 min. Data are means ± S.E. (n = 3) of a representative of three independent experiments with similar results.

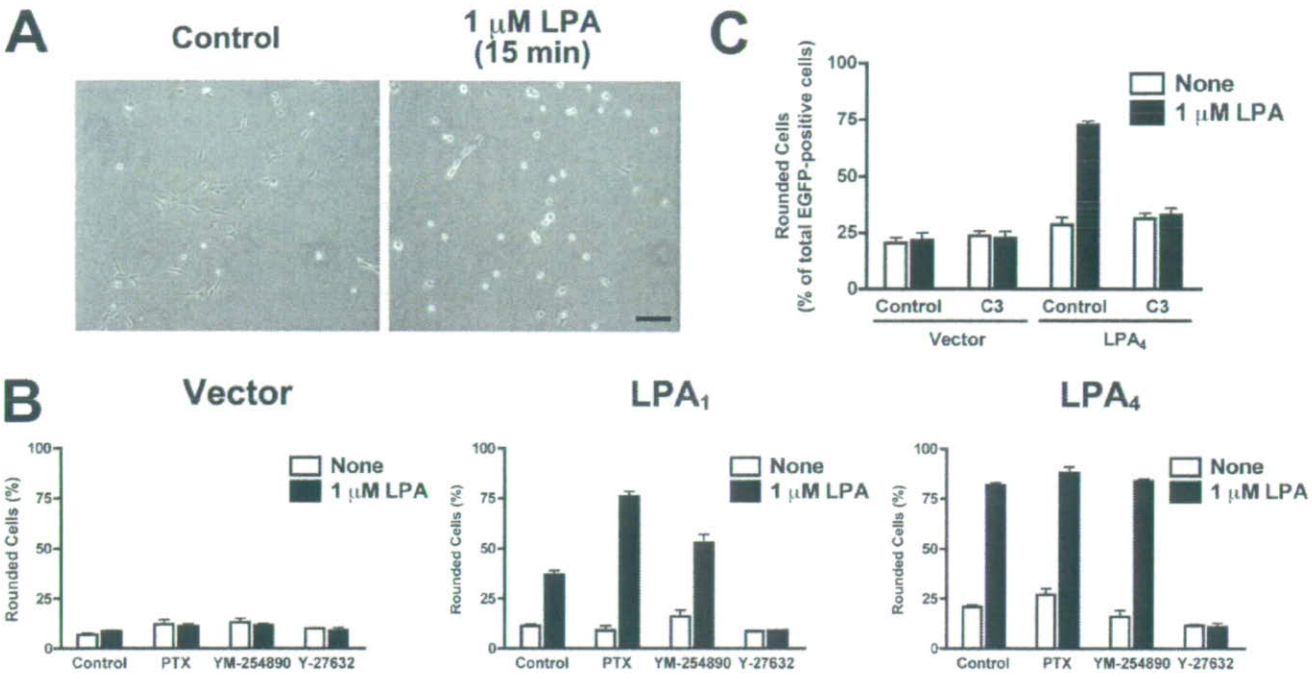

FIGURE 4. **LPA induces cell rounding in B103-LPA_4 cells through a $G_{12/13}$-Rho-ROCK-dependent pathway.** *A*, induction of cell rounding in B103-LPA_4 cells. Serum-starved B103-LPA_4 cells were stimulated with 1 μM LPA for 15 min. *Bar*, 100 μm. *B*, effects of PTX, YM-254890, and Y-27632 on LPA-induced cell rounding in B103-vector, B103-LPA_1, and B103-LPA_4 cells. The cells were pretreated with either 100 ng/ml PTX for 24 h, 5 μM YM-254890 for 10 min, or 5 μM Y-27632 for 10 min. The percentages of rounded cells among >200 cells are shown. Data are means ± S.E. (n = 3) of a representative of three independent experiments with similar results. *C*, effects of C3 exoenzyme on LPA-induced cell rounding in B103-LPA_4 cells. Either the C3 exoenzyme expression vector or the corresponding control vector was cotransfected with the EGFP expression vector. The cells were seeded, serum-starved, and treated with 1 μM LPA for 15 min. Following the fixation, EGFP images were obtained using a fluorescence microscope. The percentages of rounded cells among >100 EGFP-positive cells are shown. Data are means ± S.E. (n = 3) of a representative of two independent experiments with similar results.

(10). Mouse LPA_1 and LPA_2 and human LPA_1 have been reported to mediate LPA-induced cell rounding in B103 cells (29, 30, 33); we examined whether human LPA_4 also mediates cell rounding in B103 cells by seeding cells at a low cell density (Fig. 4, *A* and *B*). Overexpression of LPA_1 and LPA_4 slightly increased the percentages of rounded cells even before LPA application. Within 15 min of LPA stimulation, about 80% of B103-LPA_4 cells became rounded and underwent neurite retraction (Fig. 4*A*). Cell rounding was observed in B103-LPA_1 cells as reported previously (33), but to a lesser degree than in B103-LPA_4 cells. LPA-induced cell rounding was not observed in B103-vector cells.

The role of Rho in LPA-induced cell rounding is now well established (36), and the $G_{12/13}$ types of heterotrimeric G proteins are known to be upstream activators of Rho proteins (1, 2, 7). On the other hand, there are reports that $G_{q/11}$ activation induces cell rounding through Rho-dependent (37) and -independent (38) pathways. To determine which G proteins and signaling molecules are involved in LPA-induced cell rounding, we pretreated the cells with PTX, YM-254890, and a ROCK inhibitor, Y-27632 (Fig. 4*B*). In B103-LPA_4 cells, neither PTX nor YM-254890 inhibited LPA-induced cell rounding; in contrast, Y-27632 completely inhibited this morphological change. Y-27632 also hampered LPA-induced cell rounding in B103-LPA_1 cells, whereas YM-254890 did not affect the number of rounded cells. Interestingly, pretreatment with PTX increased the degree of LPA-induced cell rounding in B103-LPA_1 cells. To confirm the involvement of Rho, B103-LPA_4 cells were transfected with C3 exoenzyme, which inactivates Rho by ADP-ribosylation. The transfected cells were identified by cotransfection of an EGFP expression construct. C3 exoenzyme transfection blunted LPA-induced cell rounding in B103-LPA_4 cells, again indicating the involvement of Rho (Fig. 4*C*).

LPA_4 Mediates ROCK-dependent Cell Aggregation—As described earlier, B103-LPA_4 cells appeared to form aggregates in serum-containing medium to a greater extent than B103-vector cells (Fig. 1*B*). To determine whether the binding of LPA to LPA_4 mediates the induction of cell-cell adhesion, B103-LPA_4 cells at a medium cell density were stimulated with 1 μM LPA after 24 h of serum starvation. Although the rapid cell rounding after LPA application was difficult to evaluate at this cell density because of the formation of cell-cell contacts, LPA caused a slow but dramatic aggregation in B103-LPA_4 cells (Fig. 5*A*, *panel f*). The morphological change observed in B103-LPA_4 cells was transient, reaching a maximum 2–3 h after the treatment and then returning to the base line 24 h after the treatment (data not shown).

To investigate the signaling pathways downstream of LPA_4 that are involved in the cell aggregation, we treated B103-LPA_4 cells with several inhibitors. The LPA-induced morphological changes in B103-LPA_4 cells were completely prevented by Y-27632 (Fig. 5*A*, *panel o*). In contrast, neither PTX nor YM-254890 inhibited the cell aggregation (Fig. 5*A*, *panels i* and *l*). We quantified the degree of cell aggregation by examining the randomness in the spatial distribution of the cells (see the "Experimental Procedures"; Fig. 5*B*). These results suggest that

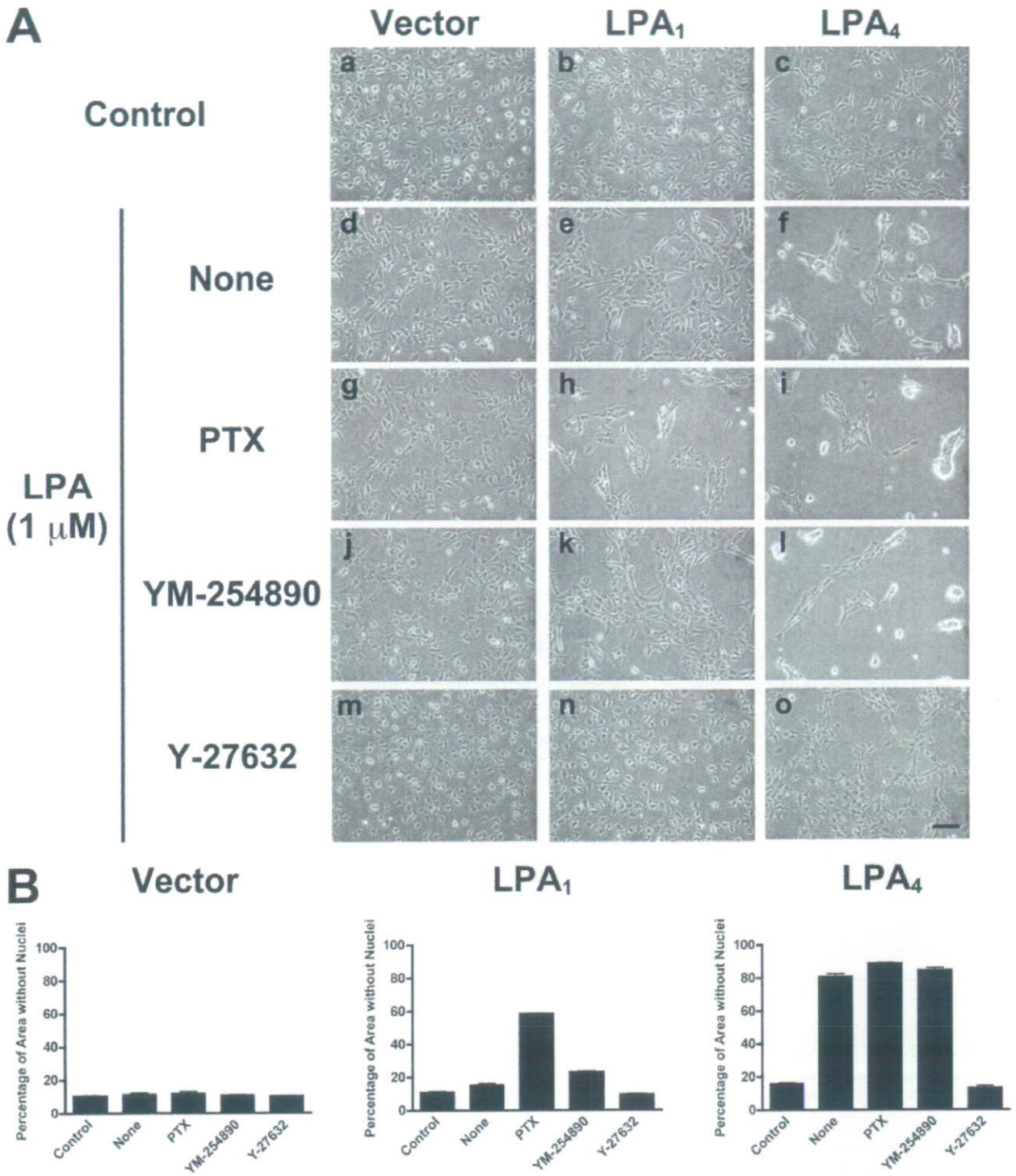

FIGURE 5. **Cell aggregation in B103-LPA_4 cells is mediated by ROCK.** *A*, cells were pretreated with either 100 ng/ml PTX for 24 h, 5 μM YM-254890 for 10 min, or 5 μM Y-27632 for 10 min prior to the LPA stimulation for 3 h. *Bar*, 100 μm. *B*, quantification of cell clustering. Serum-starved cells were treated with 1 μM LPA for 3 h, followed by fixation and staining. The intensity of the cell clustering was calculated as described under the "Experimental Procedures." Data are means ± S.E. of three different rectangular areas (one rectangular area/well) of two independent experiments with similar results.

Rho mediates LPA-induced cell aggregation in B103-LPA_4 cells in a $G_{i/o}$- and $G_{q/11}$-independent manner. Rho regulates the reorganization of the actin cytoskeleton, which can modify the intensity of adhesion (28, 39). To examine whether the reorganization of the actin cytoskeleton was involved in this effect, B103-LPA_4 cells were pretreated with cytochalasin D (an inhibitor of actin polymerization). In these cells, morphological changes were not observed after LPA stimulation, indicating that actin reorganization is involved in the LPA-induced cell aggregation (data not shown). Like B103-LPA_4 cells, PTX-

treated B103-LPA_1 cells became aggregated after LPA stimulation (Fig. 5*A*, *panel h*).

LPA_4 Mediates N-cadherin-dependent Cell-Cell Adherence—Through LPA-induced cell aggregation, B103-LPA_4 cells formed tightly compact aggregates (Fig. 5*A*, *panel f*), which dissociated very little after pipetting (data not shown). Cell-cell adhesion mechanisms can be Ca^{2+}-dependent and Ca^{2+}-independent, and cadherins are the major components of the Ca^{2+}-dependent system. Cadherin-dependent adhesion was originally defined as being trypsin-resistant in the presence of Ca^{2+} and trypsin-sensitive in the absence of Ca^{2+} (40). We examined whether LPA-induced cell adhesion was mediated by cadherins using a cell dissociation assay, one of the adhesion assays for the evaluation of the cadherin activity (27, 28). We defined the TC/TE index as a ratio of the cell particle number after trypsin treatment in the presence of Ca^{2+} (TC) to the number after trypsin treatment with EDTA (TE). Cadherin-dependent adhesion remains after trypsin-Ca^{2+} treatment, whereas trypsin-EDTA treatment disrupts cell adhesion nearly completely. In either treatment, an increase in particles would occur when a large aggregate breaks into small particles by pipetting; the higher the number of particles, the lower the aggregation (adhesion). Thus, the TC/TE index is negatively correlated with cadherin-mediated adhesion. The aggregation level of B103-LPA_4 cells increased after LPA stimulation (Fig. 6*A*; note that the index inversely reflects cadherin activity). LPA treatment did not significantly affect the TC/TE index in either B103-vector cells or B103-LPA_1 cells. These results suggest that LPA increased the cadherin-mediated adhesive activity in B103-LPA_4 cells. Even LPA-untreated B103-LPA_4 cells had significantly more cadherin-dependent adhesion activity, *i.e.* a lower TC/TE index, than LPA-untreated B103-vector and B103-LPA_1 cells (Fig. 6*A*).

The cadherins constitute a large superfamily of molecules that includes the classic cadherins, the desmosomal cadherins, the protocadherins, and the cadherin-like signaling receptors (41). The levels of the two classic cadherins most commonly expressed in the nervous system, N- and E-cadherin, were determined by Western blotting of LPA-treated or -untreated B103 cells. Consistent with a previous report (42), these cells abundantly expressed N-cadherin (Fig. 6*B*), whereas E-cadherin was undetectable (data not shown). The expression level of N-cadherin was not up-regulated by LPA treatment in any of the transfected cell lines (Fig. 6*B*), and N-cadherin was intact in the cells undergoing TC treatment. In contrast, TE treatment resulted in complete digestion of N-cadherin (data not shown), as reported previously (43). We next examined whether LPA increases N-cadherin-mediated cell-cell contacts. LPA promoted the assembly of N-cadherin in the form of a thick, bright band at the cell-cell contact area in B103-LPA_4 cells but not in B103-vector cells (Fig. 6*C*).

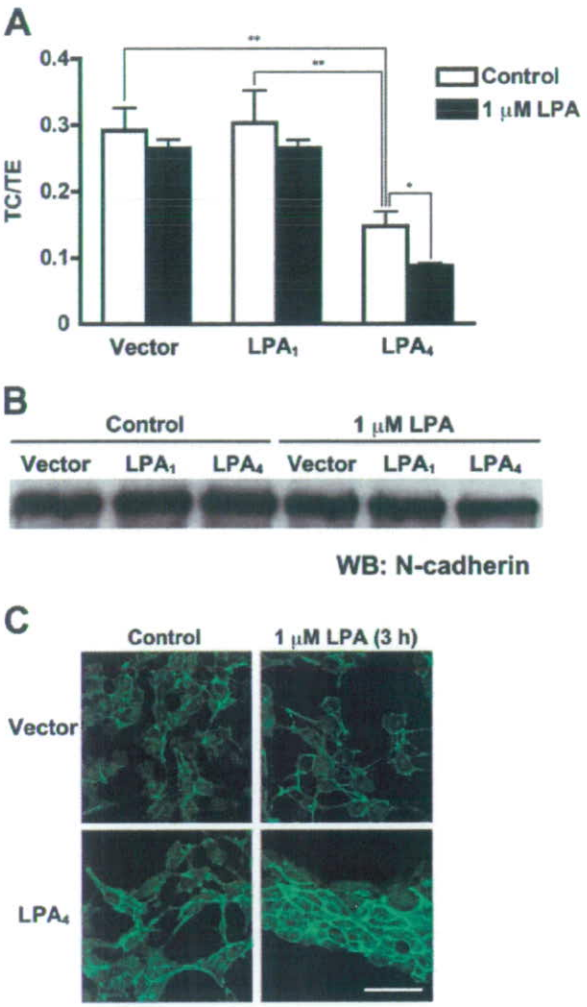

FIGURE 6. **LPA induces N-cadherin-dependent cell adhesion in B103-LPA_4 cells.** *A*, Ca^{2+} dependence of cell-cell adhesion in B103-LPA_4 cells. Serum-starved cells were stimulated with 1 μM LPA for 2 h and washed with HBSS containing either 1 mM Ca^{2+} or 1 mM EDTA. The washed cells were treated with 0.01% trypsin for 30 min in the presence of either Ca^{2+} (TC treatment) or EDTA (TE treatment) at 37 °C. Then the cells were dissociated by pipetting 10 times, and the number of particles was counted with a particle counter. The degree of cell-cell adhesion was expressed as the ratio of TC/TE. Note that the ratio inversely reflects cadherin activity. Negative control experiments without LPA treatment were also performed. Data are means ± S.E. of five independent experiments. *, $p < 0.05$; **, $p < 0.001$ (using analysis of variance followed by Tukey-Kramer test). *B*, expression of N-cadherin protein in B103 cells. Serum-starved cells were incubated with or without 1 μM LPA for 3 h and lysed. The same amount of protein was subjected to Western blot (*WB*) analysis. *C*, immunostaining of N-cadherin in B103-vector and B103-LPA_4 cells. Serum-starved cells were stimulated with 1 μM LPA, stained with an antibody against N-cadherin, and visualized with a fluorescein-labeled secondary antibody. Negative control experiments without LPA treatment were also performed. *Bar*, 100 μm.

DISCUSSION

A number of studies have shown that LPA mediates morphological changes in neuronal cells through the Rho-ROCK pathway (10, 11, 44). It has been proposed that these effects are mediated by LPA_1 and/or LPA_2 (10, 11, 44). Recently, we identified $p2y_9$/GPR23 as a fourth LPA receptor (LPA_4) that is structurally distinct from the EDG family of LPA receptors (19). The expression of LPA_4 in neuronal cells implies a significant role for this receptor in the nervous system (18). The results in this study demonstrate that LPA_4 caused morphological changes in B103 neuronal cells, including cell rounding and N-cadherin-associated cell aggregation, both of which were mediated by the Rho-ROCK pathway.

Ca^{2+} mobilization and adenylyl cyclase inhibition are the major cellular responses to LPA (45). When expressed in B103

neuronal cells, each of the EDG family LPA receptors, LPA_1, LPA_2, and LPA_3, mediates both of these reactions (30). LPA_1 is likely to mediate the Ca^{2+} response through $G_{q/11}$ proteins (Fig. 3). The PTX-sensitive inhibition of adenylyl cyclase (Fig. 2*A*) suggests that LPA_1 also couples to $G_{i/o}$. We showed that LPA_4 mediates the Ca^{2+} response in B103 cells (Fig. 3). This is consistent with our previous report (19) that the stable expression of LPA_4 in Chinese hamster ovary cells significantly enhanced the LPA-induced Ca^{2+} mobilization. From our results using YM-254890, LPA_4 probably mediates Ca^{2+} mobilization through $G_{q/11}$ proteins (Fig. 3). In contrast, LPA did not inhibit adenylyl cyclase in B103-LPA_4 cells (Fig. 2*A*). These results indicate that unlike the other LPA receptor subtypes, LPA_4 does not couple to $G_{i/o}$ proteins.

Neurite retraction and neurite formation play a role in the remodeling of neurons for guidance and synaptic plasticity (46). Neurite retraction in neuronal cells is induced by lysophospholipids, including LPA and sphingosine 1-phosphate (S1P), in addition to semaphorins, netrins, and ephrins (10, 11, 47). LPA induces neurite retraction through LPA_1 or LPA_2 when expressed in B103 cells (30). In this study, we showed that 1 μM LPA induced cell rounding in B103-LPA_4 cells (Fig. 4*A*). Sugiura *et al.* (48) reported that rat brain contains 3.73 nmol of LPA/g of tissue. These results suggest a role for LPA_4 in LPA-induced neurite retraction. Neurite initiation and formation involve actin cytoskeletal changes, and as a regulator of actin reorganization, Rho GTPase has a profound effect on neuritogenesis (47). For example, S1P induces Rho-dependent neurite retraction through the $S1P_2$ (49, 50), $S1P_3$ (49), and $S1P_5$ receptors (50, 51). Several studies have also revealed a critical role for Rho and ROCK in LPA-induced neurite retraction (36, 52, 53), although some studies have reported Rho-independent neurite retraction (38, 54). Judging from its complete inhibition by C3 exoenzyme and Y-27632, the cell rounding induced by LPA_4 depended on Rho and ROCK in B103-LPA_4 cells (Fig. 4, *B* and *C*).

In general, activation of $G_{12/13}$ proteins leads to an increase in RhoA guanine nucleotide exchange, activation of ROCK, and actin polymerization (55, 56), although some studies have implied that $G_{q/11}$ proteins can also activate Rho (57, 58). Based on our results, it is conceivable that the $G_{12/13}$ proteins are upstream regulators of Rho in B103-LPA_1 cells and B103-LPA_4 cells, because YM-254890 inhibited cell rounding in both cell types (Fig. 4*B*). In many studies reporting the induction of neurite retraction by LPA (10), the LPA receptor subtypes responsible have not been identified, or LPA_1 and LPA_2 were suggested as candidate subtypes based on mRNA expression in the neuronal cells examined (59–62). This study suggests the possibility that LPA_4 was involved in the neurite retraction in some of these studies.

LPA has been shown to stimulate cell motility and to modulate tumor cell invasion, both of which are mediated mainly by LPA_1 and $G_{i/o}$ proteins (33, 63, 64). In the presence of serum, B103-LPA_1 cells exhibited a flattened morphology and were widely dispersed throughout the dish (Fig. 1*B*) (33). This morphological phenotype was probably evoked by LPA through the LPA_1-$G_{i/o}$-Rac signaling axis (33). In sharp contrast to B103-LPA_1 cells, B103-LPA_4 cells formed cell aggregates in serum-containing medium (Fig. 1*B*), apparently through activation of the $G_{12/13}$-Rho-ROCK signaling axis (Fig. 5). This cell-cell adhesion involved N-cadherin without *de novo* synthesis (Fig. 6). Because Rho affects cadherin-dependent adhesion through actin cytoskeleton reorganization (28), we presume that LPA-induced cytoskeletal changes affect the subcellular distribution of N-cadherin, as shown in Fig. 6*C*, leading to strong cell-cell adhesion in B103-LPA_4 cells. This is supported by the current results that treatment with Y-27632 and cytochalasin D abolished the LPA-induced cell aggregation (Fig. 5 and data not shown). N-cadherin is widely expressed in the nervous system and has critical roles in neural development and functions, including synapse formation and myelination. Weiner *et al.* (65) previously reported that LPA induced cell-cell junctions containing N-cadherin in rat Schwann cells. Furthermore, LPA was reported to induce cell clustering in neural progenitor cells prepared from embryonic rat hippocampus (66) and in mouse postmitotic cortical neurons (16). Our results raise the possibility that in addition to LPA_1 and LPA_2, LPA_4 might also be involved in these effects in neural cells and have critical roles in the development and function of the nervous system. In contrast to LPA_1 and LPA_2, which activate Rac through $G_{i/o}$ (17, 64), LPA_4 is unlikely to activate the $G_{i/o}$-Rac pathway because LPA_4 did not inhibit adenylyl cyclase activity (Fig. 3*A*). Therefore, LPA_4 might have a unique role in keeping a proper balance between Rho and Rac activation, which is important for neuronal development and function (47).

We observed that PTX significantly enhanced the intensity of LPA_1-mediated cell rounding (Fig. 4*B*). This "permissive effect" is consistent with a previous report that PTX enables LPA-induced cell rounding in 1321N1 astrocytoma cells (61). It is known that Rho activity is inhibited by Rac activation through $G_{i/o}$ proteins (67). Indeed, Rac activation functionally antagonizes Rho-mediated neurite retraction in 1321N1 astrocytoma cells (61). LPA_1 was shown to couple to $G_{i/o}$ and activate Rac strongly in B103 cells (33) and other cells, including mouse embryonic meningeal fibroblast (MEMF) and mouse skin fibroblast (MSF) cells (17, 64). Taken together, we suggest that PTX treatment of B103-LPA_1 cells suppresses $G_{i/o}$ proteins and subsequently suppresses Rac activation by LPA, which in turn permits Rho-mediated cell rounding. This mechanism probably also accounts for the LPA-induced aggregation of PTX-treated B103-LPA_1 cells (Fig. 5, *A*, *panel h*, and *B*).

We showed here that LPA_4 has Rho-dependent morphological effects. It has been reported that LPA-induced Rho activation is mediated by LPA_1 and/or LPA_2. However, pathways independent of LPA_1 and LPA_2 have also been proposed. Contos *et al.* (17) showed that MEMF cells from LPA_1 and LPA_2 double knockouts remained capable of forming stress fibers in response to LPA. This study proposed the presence of unknown LPA receptors in MEMF cells because of the absence of LPA_3 mRNA. Consistent with this, Hama *et al.* (64) reported that LPA activates Rho in MSF cells from LPA_1 and LPA_2 double knockouts. Our results, together with the abundant expression of LPA_4 in MSF cells (64), suggest that LPA_4 may also be involved in LPA-induced Rho activation in these cells. Furthermore, Hama *et al.* (64) observed that Rac activation was totally

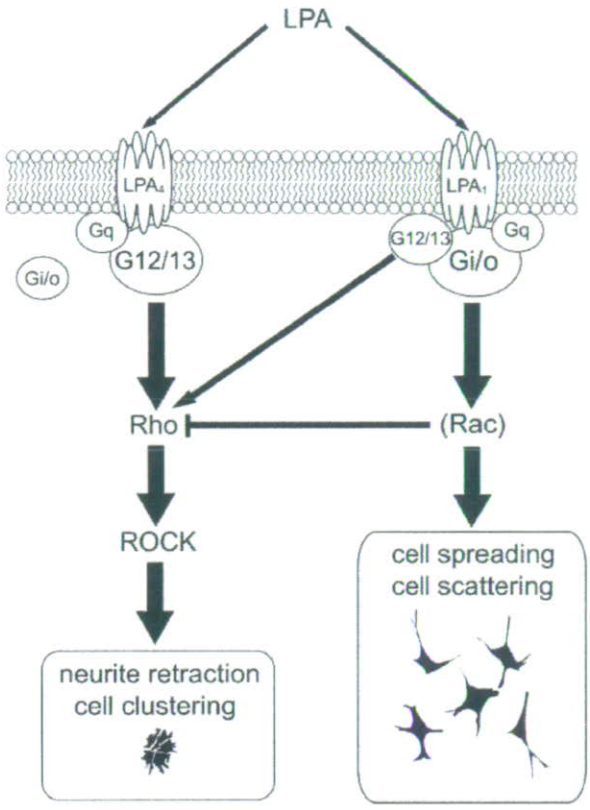

FIGURE 7. **LPA_1 and LPA_4 have distinct signaling pathways that produce different cell morphologies in B103 cells.** LPA_4 expression results in cell rounding and aggregated morphology through $G_{12/13}$-Rho-ROCK pathway. In contrast, LPA_1 expression results in flattened and dispersed morphology as reported previously (33). Inactivation of $G_{i/o}$ proteins in LPA_1-expressing cells by PTX treatment leads to "LPA_4-expressing cells like" aggregated morphology, suggesting the involvement of the inhibitory effect of $G_{i/o}$ on Rho activation probably through Rac. Both LPA_1 and LPA_4 couple to G_q, although G_q-involved pathway does not affect cell morphology.

dependent on LPA_1 and LPA_2, supporting our hypothesis that LPA_4 does not activate the $G_{i/o}$-Rac signaling axis.

We also observed that the stable expression of LPA_1 or LPA_4 slightly increased the population of rounded cells even before LPA application (Fig. 4*B*). Furthermore, serum-starved B103-LPA_4 cells adhered to one another more strongly than B103-vector or B103-LPA_1 cells did (Fig. 6*A*). These morphological effects might be because of the constitutive activation of these LPA receptors. Indeed, there are many reports showing that the constitutive expression of GPCR for lipid mediators, including lysophospholipids and prostanoids, has morphological effects (30, 49, 68, 69). For example, cell rounding and cadherin-dependent adhesion in the absence of ligand occur in human embryonic kidney 293 cells transfected with FP_B receptor, an isoform of prostanoid GPCR (69, 70). The involvement of phosphatidylinositol 3-kinase and β-catenin was proposed for these constitutive activities (70). Another conceivable explanation for the morphological effects observed in serum-starved B103-LPA_1 and B103-LPA_4 cells involves autocrine ligand secretion and subsequent receptor activation (33). Both hypotheses are consistent with our results that the treatment of these cells with Y-27632 decreased the percentage of rounded cells (Fig. 4*B*).

LPA_4 Changes the Morphology of Neuronal Cells

In summary, as shown in Fig. 7, we demonstrate for the first time that the novel LPA receptor subtype LPA_4 is coupled to the activation of Rho in a rat neuronal cell line. The activation of Rho through LPA_4 leads to morphological changes, including cell rounding and cell aggregation. LPA is well known to induce neurite retraction and cell clustering in neural cells. The identification of Rho as an effector of LPA_4 will give insight into some of the physiological and morphological effects of LPA that could not be explained by the EDG family LPA receptors. A full understanding of the potential roles of the endogenous LPA_4 receptor in the development and function of the nervous system awaits future studies.

Acknowledgments—We thank Drs. T. Yokomizo and T. Okuno (Kyushu University) for vital discussions and critical suggestions. We also thank Dr. J. Chun (The Scripps Research Institute, La Jolla, CA) for providing B103 rat neuroblastoma cells; Dr. J. Miyazaki (Osaka University) for pCXN2; Drs. S. Narumiya (Kyoto University) and S. Nagata (Osaka University) for the expression vector for C3 exoenzyme (pEF-C3) and its parental vector (pEF-BOS), respectively; and Dr. J. Takasaki (Astellas Pharma, Tokyo, Japan) for YM-254890.

REFERENCES

1. Moolenaar, W. H., van Meeteren, L. A., and Giepmans, B. N. (2004) *BioEssays* **26,** 870–881
2. Anliker, B., and Chun, J. (2004) *J. Biol. Chem.* **279,** 20555–20558
3. Hecht, J. H., Weiner, J. A., Post, S. R., and Chun, J. (1996) *J. Cell Biol.* **135,** 1071–1083
4. An, S., Bleu, T., Zheng, Y., and Goetzl, E. J. (1998) *Mol. Pharmacol.* **54,** 881–888
5. Bandoh, K., Aoki, J., Hosono, H., Kobayashi, S., Kobayashi, T., Murakami-Murofushi, K., Tsujimoto, M., Arai, H., and Inoue, K. (1999) *J. Biol. Chem.* **274,** 27776–27785
6. Contos, J. J., Ishii, I., and Chun, J. (2000) *Mol. Pharmacol.* **58,** 1188–1196
7. Ishii, I., Fukushima, N., Ye, X., and Chun, J. (2004) *Annu. Rev. Biochem.* **73,** 321–354
8. Das, A. K., and Hajra, A. K. (1989) *Lipids* **24,** 329–333
9. Tokumura, A. (1995) *Prog. Lipid Res.* **34,** 151–184
10. Ye, X., Fukushima, N., Kingsbury, M. A., and Chun, J. (2002) *Neuroreport* **13,** 2169–2175
11. Chun, J. (2005) *Prostaglandins Other Lipid Mediat.* **77,** 46–51
12. Contos, J. J., Fukushima, N., Weiner, J. A., Kaushal, D., and Chun, J. (2000) *Proc. Natl. Acad. Sci. U. S. A.* **97,** 13384–13389
13. Harrison, S. M., Reavill, C., Brown, G., Brown, J. T., Cluderay, J. E., Crook, B., Davies, C. H., Dawson, L. A., Grau, E., Heidbreder, C., Hemmati, P., Hervieu, G., Howarth, A., Hughes, Z. A., Hunter, A. J., Latcham, J., Pickering, S., Pugh, P., Rogers, D. C., Shilliam, C. S., and Maycox, P. R. (2003) *Mol. Cell. Neurosci.* **24,** 1170–1179
14. Inoue, M., Rashid, M. H., Fujita, R., Contos, J. J., Chun, J., and Ueda, H. (2004) *Nat. Med.* **10,** 712–718
15. Kingsbury, M. A., Rehen, S. K., Contos, J. J., Higgins, C. M., and Chun, J. (2003) *Nat. Neurosci.* **6,** 1292–1299
16. Fukushima, N., Weiner, J. A., Kaushal, D., Contos, J. J., Rehen, S. K., Kingsbury, M. A., Kim, K. Y., and Chun, J. (2002) *Mol. Cell. Neurosci.* **20,** 271–282
17. Contos, J. J., Ishii, I., Fukushima, N., Kingsbury, M. A., Ye, X., Kawamura, S., Brown, J. H., and Chun, J. (2002) *Mol. Cell. Biol.* **22,** 6921–6929
18. Jin Rhee, H., Nam, J. S., Sun, Y., Kim, M. J., Choi, H. K., Han, D. H., Kim, N. H., and Huh, S. O. (2006) *Neuroreport* **17,** 523–526
19. Noguchi, K., Ishii, S., and Shimizu, T. (2003) *J. Biol. Chem.* **278,** 25600–25606
20. Janssens, R., Boeynaems, J. M., Godart, M., and Communi, D. (1997) *Biochem. Biophys. Res. Commun.* **236,** 106–112
21. O'Dowd, B. F., Nguyen, T., Jung, B. P., Marchese, A., Cheng, R., Heng, H. H., Kolakowski, L. F., Jr., Lynch, K. R., and George, S. R. (1997) *Gene*

(*Amst.*) **187,** 75–81
22. Fujiwara, Y., Sebok, A., Meakin, S., Kobayashi, T., Murakami-Murofushi, K., and Tigyi, G. (2003) *J. Neurochem.* **87,** 1272–1283
23. Takasaki, J., Saito, T., Taniguchi, M., Kawasaki, T., Moritani, Y., Hayashi, K., and Kobori, M. (2004) *J. Biol. Chem.* **279,** 47438–47445
24. Niwa, H., Yamamura, K., and Miyazaki, J. (1991) *Gene* (*Amst.*) **108,** 193–199
25. Fujisawa, K., Madaule, P., Ishizaki, T., Watanabe, G., Bito, H., Saito, Y., Hall, A., and Narumiya, S. (1998) *J. Biol. Chem.* **273,** 18943–18949
26. Mizushima, S., and Nagata, S. (1990) *Nucleic Acids Res.* **18,** 5322
27. Nagafuchi, A., Ishihara, S., and Tsukita, S. (1994) *J. Cell Biol.* **127,** 235–245
28. Fukata, M., Kuroda, S., Nakagawa, M., Kawajiri, A., Itoh, N., Shoji, I., Matsuura, Y., Yonehara, S., Fujisawa, H., Kikuchi, A., and Kaibuchi, K. (1999) *J. Biol. Chem.* **274,** 26044–26050
29. Fukushima, N., Kimura, Y., and Chun, J. (1998) *Proc. Natl. Acad. Sci. U. S. A.* **95,** 6151–6156
30. Ishii, I., Contos, J. J., Fukushima, N., and Chun, J. (2000) *Mol. Pharmacol.* **58,** 895–902
31. Tsukahara, T., Tsukahara, R., Yasuda, S., Makarova, N., Valentine, W. J., Allison, P., Yuan, H., Baker, D. L., Li, Z., Bittman, R., Parrill, A., and Tigyi, G. (2006) *J. Biol. Chem.* **281,** 3398–3407
32. Bockaert, J., and Pin, J. P. (1999) *EMBO J.* **18,** 1723–1729
33. van Leeuwen, F. N., Olivo, C., Grivell, S., Giepmans, B. N., Collard, J. G., and Moolenaar, W. H. (2003) *J. Biol. Chem.* **278,** 400–406
34. Meyer Zu Heringdorf, D. (2004) *J. Cell. Biochem.* **92,** 937–948
35. von Kugelgen, I. (2006) *Pharmacol. Ther.* **110,** 415–432
36. Jalink, K., van Corven, E. J., Hengeveld, T., Morii, N., Narumiya, S., and Moolenaar, W. H. (1994) *J. Cell Biol.* **126,** 801–810
37. Katoh, H., Aoki, J., Yamaguchi, Y., Kitano, Y., Ichikawa, A., and Negishi, M. (1998) *J. Biol. Chem.* **273,** 28700–28707
38. Couvillon, A. D., and Exton, J. H. (2006) *Cell. Signal.* **18,** 715–728
39. Hall, A. (1998) *Science* **279,** 509–514
40. Takeichi, M. (1977) *J. Cell Biol.* **75,** 464–474
41. Gumbiner, B. M. (2005) *Nat. Rev. Mol. Cell Biol.* **6,** 622–634
42. Chen, Q., Chen, T. J., Letourneau, P. C., Costa Lda, F., and Schubert, D. (2005) *J. Neurosci.* **25,** 281–290
43. Wanner, I. B., and Wood, P. M. (2002) *J. Neurosci.* **22,** 4066–4079
44. Fukushima, N. (2004) *J. Cell. Biochem.* **92,** 993–1003
45. Tigyi, G. (2001) *Prostaglandins Other Lipid Mediat.* **64,** 47–62
46. Luo, L., and O'Leary, D. D. (2005) *Annu. Rev. Neurosci.* **28,** 127–156
47. Govek, E. E., Newey, S. E., and Van Aelst, L. (2005) *Genes Dev.* **19,** 1–49
48. Sugiura, T., Nakane, S., Kishimoto, S., Waku, K., Yoshioka, Y., Tokumura, A., and Hanahan, D. J. (1999) *Biochim. Biophys. Acta* **1440,** 194–204
49. van Brocklyn, J. R., Tu, Z., Edsall, L. C., Schmidt, R. R., and Spiegel, S. (1999) *J. Biol. Chem.* **274,** 4626–4632
50. Toman, R. E., Payne, S. G., Watterson, K. R., Maceyka, M., Lee, N. H., Milstien, S., Bigbee, J. W., and Spiegel, S. (2004) *J. Cell Biol.* **166,** 381–392
51. Jaillard, C., Harrison, S., Stankoff, B., Aigrot, M. S., Calver, A. R., Duddy, G., Walsh, F. S., Pangalos, M. N., Arimura, N., Kaibuchi, K., Zalc, B., and Lubetzki, C. (2005) *J. Neurosci.* **25,** 1459–1469
52. Hirose, M., Ishizaki, T., Watanabe, N., Uehata, M., Kranenburg, O., Moolenaar, W. H., Matsumura, F., Maekawa, M., Bito, H., and Narumiya, S. (1998) *J. Cell Biol.* **141,** 1625–1636
53. Kranenburg, O., Poland, M., van Horck, F. P., Drechsel, D., Hall, A., and Moolenaar, W. H. (1999) *Mol. Biol. Cell* **10,** 1851–1857
54. Somlyo, A. P., and Somlyo, A. V. (2000) *J. Physiol.* (*Lond.*) **522,** 177–185
55. Hart, M. J., Jiang, X., Kozasa, T., Roscoe, W., Singer, W. D., Gilman, A. G., Sternweis, P. C., and Bollag, G. (1998) *Science* **280,** 2112–2114
56. Kozasa, T., Jiang, X., Hart, M. J., Sternweis, P. M., Singer, W. D., Gilman, A. G., Bollag, G., and Sternweis, P. C. (1998) *Science* **280,** 2109–2111
57. Chikumi, H., Vazquez-Prado, J., Servitja, J. M., Miyazaki, H., and Gutkind, J. S. (2002) *J. Biol. Chem.* **277,** 27130–27134
58. Vogt, S., Grosse, R., Schultz, G., and Offermanns, S. (2003) *J. Biol. Chem.* **278,** 28743–28749
59. Sayas, C. L., Avila, J., and Wandosell, F. (2002) *J. Neurosci.* **22,** 6863–6875
60. Dawson, J., Hotchin, N., Lax, S., and Rumsby, M. (2003) *J. Neurochem.* **87,** 947–957
61. Seasholtz, T. M., Radeff-Huang, J., Sagi, S. A., Matteo, R., Weems, J. M., Cohen, A. S., Feramisco, J. R., and Brown, J. H. (2004) *J. Neurochem.* **91,** 501–512
62. Sayas, C. L., Moreno-Flores, M. T., Avila, J., and Wandosell, F. (1999) *J. Biol. Chem.* **274,** 37046–37052
63. Yamada, T., Sato, K., Komachi, M., Malchinkhuu, E., Tobo, M., Kimura, T., Kuwabara, A., Yanagita, Y., Ikeya, T., Tanahashi, Y., Ogawa, T., Ohwada, S., Morishita, Y., Ohta, H., Im, D. S., Tamoto, K., Tomura, H., and Okajima, F. (2004) *J. Biol. Chem.* **279,** 6595–6605
64. Hama, K., Aoki, J., Fukaya, M., Kishi, Y., Sakai, T., Suzuki, R., Ohta, H., Yamori, T., Watanabe, M., Chun, J., and Arai, H. (2004) *J. Biol. Chem.* **279,** 17634–17639
65. Weiner, J. A., Fukushima, N., Contos, J. J., Scherer, S. S., and Chun, J. (2001) *J. Neurosci.* **21,** 7069–7078
66. Harada, J., Foley, M., Moskowitz, M. A., and Waeber, C. (2004) *J. Neurochem.* **88,** 1026–1039
67. Burridge, K., and Wennerberg, K. (2004) *Cell* **116,** 167–179
68. Hasegawa, H., Negishi, M., Katoh, H., and Ichikawa, A. (1997) *Biochem. Biophys. Res. Commun.* **234,** 631–636
69. Pierce, K. L., Fujino, H., Srinivasan, D., and Regan, J. W. (1999) *J. Biol. Chem.* **274,** 35944–35949
70. Fujino, H., Srinivasan, D., and Regan, J. W. (2002) *J. Biol. Chem.* **277,** 48786–48795

Eosinophil Trans-Basement Membrane Migration Induced by Interleukin-8 and Neutrophils

Izumi Kikuchi, Shinya Kikuchi, Takehito Kobayashi, Koichi Hagiwara, Yoshio Sakamoto, Minoru Kanazawa, and Makoto Nagata

Department of Respiratory Medicine, Saitama Medical School, Saitama, Japan; and Department of Allergy and Respiratory Medicine, Kanto Central Hospital of the Mutual Aid Association of Public School Teachers, Tokyo, Japan

Neutrophilic inflammation observed with severe asthma is often associated with interleukin-8 (IL-8). Neutrophils can secrete a variety of mediators that may augment the migration of eosinophils. We have reported a positive correlation between the concentrations of neutrophils and eosinophils in sputum from subjects with severe asthma, suggesting a possible role of neutrophils in regulating eosinophilic inflammation. The aim of this study was to investigate whether neutrophils stimulated with IL-8 modify the trans-basement membrane migration (TBM) of eosinophils. Eosinophils and neutrophils were isolated from peripheral blood drawn from healthy donors or subjects with mild asthma. The TBM of eosinophils in response to IL-8 was evaluated in the presence or absence of neutrophils using the chambers with a Matrigel-coated transwell insert. Neither IL-8 alone nor the presence of neutrophils alone induced the TBM of eosinophils. However, when eosinophils were coincubated with neutrophils and stimulated with IL-8, the TBM of eosinophils was significantly augmented. This augmented TBM of eosinophils was inhibited by a matrix metalloproteinase-9 inhibitor, a leukotriene B_4 receptor antagonist, platelet-activating factor antagonists, or an anti–TNF-α monoclonal antibodies. These results suggest that neutrophils migrated in response to IL-8 may lead eosinophils to accumulate in the airways of asthma and possibly aggravate this disease.

Keywords: eosinophils; growth-related oncogene-α; interleukin-8; neutrophils; trans-basement membrane migration

Eosinophils, inflammatory cells predominantly found in the airways of patients with asthma, likely contribute to airway remodeling or airflow limitation observed with asthma (1–4). The mechanism by which eosinophils accumulate in the airways is a complex process that is mainly regulated by cytokines, chemokines, and adhesion molecules. This process is likely to be inhibited by corticosteroid treatment via the suppression of cytokines/chemokines productions from corticosteroid-sensitive cells such as Th2 cells. In a subgroup of patients, accumulation of neutrophils is found in their airways even in the absence of apparent infection. Asthma in such patients is often severe and chronic and is refractory to corticosteroid therapy (5–8). Based on a recent report from the European network study for understanding mechanisms of severe asthma (ENFUMOSA), patients with severe asthma have greater sputum neutrophilia and evidence of ongoing eosinophil-derived mediator release, compared with patients with mild to moderate asthma, suggesting that both neutrophilic and eosinophilic inflammation persists in the airways of severe asthma (9). In this context, we have recently reported a positive correlation between the concentrations of neutrophils and eosinophils in induced sputum from patients with severe persistent asthma who are treated with medicines including systemic corticosteroid (10).

Functions of neutrophils are not effectively suppressed by corticosteroids (11, 12), suggesting that neutrophils may play a role in the pathophysiology of the disease in such patients. There are many reports which suggest that neutrophils are exposed to a variety of inflammatory mediators in the airways of patients with asthma. For example, interleukin-8 (IL-8), which acts as a chemoattractant for neutrophils, is found in bronchoalveolar lavage fluid and serum from patients with asthma (13–16). Concentration of IL-8 has been shown to be correlated with accumulation of neutrophils in the airways of asthma (6), and therefore this chemokine may be an essential molecule responsible for the development of neutrophilic inflammation in asthma. Activated neutrophils can secrete a variety of mediators (e.g., matrix metalloproteinases [MMPs], leukotriene B_4 [LTB_4], platelet-activating factor [PAF], and TNF-α) that can induce digestion of basement membrane, or migration or activation of eosinophils (17, 18), and may thus contribute to the pathophysiology of asthma.

We framed a hypothesis that neutrophils stimulated with and migrated to IL-8 play roles in the regulation of eosinophilic inflammation in asthma. Trans-basement membrane migration (TBM) is one of the key processes by which circulating eosinophils accumulate in the airways of asthma. Here we report that a combination of IL-8 and neutrophils augment the TBM of eosinophils.

MATERIALS AND METHODS

Reagents

Anti-CD16 antibody–coated magnetic beads were purchased from Miltenyi Biotec (Auburn, CA). Percoll was purchased from Pharmacia (Uppsala, Sweden). HBSS was purchased from GIBCO BRL (Grand island, NY). BIIL260, an LTB_4 receptor antagonist, and WEB2086 and WEB2170, PAF receptor antagonists, were provided by Boehringer Ingelheim (Ridgefield, CT). MMP-9 inhibitor and GM1489, an MMP inhibitor, was purchased from Calbiochem (San Diego, CA). AA861, a 5-lipoxygenase (LO) inhibitor, and PBS were obtained from Wako (Osaka, Japan). IL-8, Growth-related oncogene-α (GRO-α), TNF-α, eotaxin, regulated upon activation, normal T cell expressed and secreted (RANTES), and anti–CXC chemokine receptor 2 (CXCR2) antibody were purchased from R&D Systems (Minneapolis, MN). LTB_4 was purchased from Cayman Chemical (Ann Arbor, MI). PAF, Phorbol 12-myristate 13-acetate(PMA), *o*-phenylenediamine (OPD), and BSA were obtained from Sigma (St. Louis, MO). Anti–TNF-α monoclonal antibody (mAb) (clone Mab11, mouse IgG1) was purchased from Becton Dickinson (Franklin Lakes, NJ). Mouse IgG1, an isotype control for anti–TNF-α mAb, and newborn calf serum (NCS) were purchased from ICN Biomedicals, Inc. (Aurora, OH). The acetoxy methyl ester of 2′-7′-bis (2-carboxy-ethyl)-5(6)-carboxyfluorescein (BCECF-AM) was purchased from Dojin Laboratory (Kumamoto, Japan).

Preparation of Neutrophils and Eosinophils

Neutrophils and eosinophils were isolated from peripheral blood collected from nonatopic healthy donors whose eosinophil content was < 5% of

(Received in original form August 4, 2005 and in final form January 18, 2006)

Correspondence and requests for reprints should be addressed to Makoto Nagata M.D., Ph.D., Department of Respiratory Medicine, Saitama Medical School, Saitama, Japan. E-mail: favre4mn@saitama-med.ac.jp

Am J Respir Cell Mol Biol Vol 34. pp 760–765, 2006
Originally Published in Press as DOI: 10.1165/rcmb.2005-0303OC on February 2, 2006
Internet address: www.atsjournals.org

their peripheral leukocytes. In some experiments, cells isolated from individuals with mild intermittent asthma were also used. The numbers of males and females were comparable among donors, with similar age distributions ranging from 20–38 yr. Informed consent was obtained before collection of each blood sample. Neutrophils and eosinophils were separated by the combination of Percoll density gradient centrifugation and negative immunomagnetic bead selection as previously described (19, 20). Briefly, 40 ml of dextran were added to 160 ml of heparinized blood, and erythrocytes were removed as sediment. The remaining suspension of leukocytes was layered onto Percoll gradients of 1.080, 1.085, and 1.090 g/ml in density. After centrifugation at 700 × *g* for 20 min, neutrophils (purity exceeded 95%) were collected from 1.085/1.090 g/ml interface, and suspended in HBSS containing 0.2% BSA (HBSS/BSA buffer). After the removal of Percoll, the red blood cells in the pellet were lysed by hypotonic shock and removed by washing with cold PBS. The remaining cells were washed with 4°C HBSS supplemented with 2% NCS (HBSS/NCS), then incubated with anti-CD16 antibody–coated magnetic beads for 30 min at 4°C, and were then filtered with a column containing steel wool placed in a magnetic field (Miltenyi Biotec). Eosinophils (> 98% purity and > 99% viability), which passed through the column, were collected and washed, and the number of cells was adjusted to 2.5×10^5 cells/ml by using HBSS/BSA buffer.

TBM

The TBM of neutrophils and eosinophils was examined using a modified Boyden's chamber method (21). The study was conducted in duplicate. Briefly, neutrophils were suspended in loading buffer with BCECF-AM at a final concentration of 1 μM and incubated for 30 min at 37°C while shading the light (22, 23). The cells retain the label at least for 90 min (23) and superoxide anion generation in response to PMA (0.5ng/ml) was not modified by BCECF-AM (our unpublished observation). Labeled neutrophils (0.5×10^5 cells), eosinophils (0.5×10^5 cells), or a combination thereof (0.5×10^5 cells plus 0.5×10^5 cells) in a 200-μl medium were added to the upper compartment of a chamber with a Matrigel-coated transwell insert (pore size 3 μm; Becton Dickinson Labware). Either the control medium (500 μl) or a medium that contained one of activators (IL-8, GRO-α, eotaxin, RANTES, and LTB_4) was added to the lower compartment of the chamber. After a 2-h incubation in 5% CO_2 at 37°C, the medium in the upper compartment of the chamber and the inserts between the chambers were gently removed. The peroxidase activity of eosinophils in the medium in the lower compartment of the chamber was determined, and the number of migrated eosinophils was calculated from the activity of the standard media which contained known numbers (5×10^3, 1.5×10^4, 5×10^4, 1.5×10^5, and 5×10^5 cells) of eosinophils. To determine the peroxidase activity of eosinophils, the medium was incubated with a substrate (1 mM OPD, 1 mM H_2O_2, and 0.1% Triton X-100 in Tris-HCl, pH 8.0) for 30 min at room temperature (21). The reaction was stopped by adding 100 μl of 4N H_2SO_4, and absorbance at 490 nm was determined (21). The effect of neutrophils on the outer density value in this assay was negligible: 0.046 ± 0.002 for 0% control and 0.064 ± 0.006 for 100% control of neutrophils, respectively (n = 4). Similarly, addition of neutrophils to 100% control of eosinophils did not modify the outer density value (1.566 ± 0.023 by addition of 0% control versus 1.569 ± 0.012 by addition of 100% control of neutrophils (n = 4, P = n.s.). The numbers of migrated neutrophils were determined by the measurement of fluorescence in the medium using the Fluoromark (Bio-Rad Laboratories, Hercules, CA) microplate fluorometer (23). The number of migrated neutrophils determined by this method was highly correlated with those counted by hemocytometer (n = 13, $P < 0.001$, r = 0.9, Pearson's correlation coefficient). The viability of both eosinophils and neutrophils after migration exceeded 98% by trypan blue exclusion.

Blocking Study

Both eosinophils and neutrophils were incubated in a medium containing BIIL260, WEB2086, WEB2170 or AA861 for 15 min at 37°C, in a medium containing anti-TNF-α mAb (clone Mab11) or an isotype matched control mouse IgG1 for 15 min at ambient temperature, or in a medium containing MMP-9 inhibitor for 30 min at 37°C. The media containing the cells were then transferred to the upper compartment of the chamber, and the assay was performed as described above.

Statistical Analysis

Values are expressed as means ± SEM. Student's t test was conducted to compare two groups, and repeated-measures ANOVA with Scheffé's constants were used to compare more than two groups. A value of $P < 0.05$ was considered statistically significant.

RESULTS

Effects of Neutrophils on the TBM of Eosinophils

To investigate whether stimulated neutrophils affect the TBM of eosinophils, we coincubated a mixture of eosinophils and neutrophils in the presence or absence of IL-8, a CXC chemokine that selectively stimulates chemotactic response of neutrophils. Preliminary experiments confirmed that 10 nM of IL-8 is sufficient to induce the TBM of neutrophils (data not shown). Neither a coincubation with neutrophils nor IL-8 (10 nM) alone induced the TBM of eosinophils (migrated eosinophils: 0.9 ± 0.4% by medium control, 2.2 ± 0.8% by coincubation with neutrophils, P = n.s.; 1.9 ± 0.5% by IL-8 alone, P = n.s.; n = 10) (Figure 1). However, when eosinophils were coincubated with neutrophils and stimulated with IL-8, a significant TBM of eosinophils was observed (migrated eosinophils: 12.9 ± 3.1%, $P < 0.01$ versus the other three conditions; n = 10) (Figure 1). Checkerboard analysis confirmed that the effect of IL-8 on the TBM of eosinophils coincubated with neutrophils is chemotactic (n = 3, data not shown). When the transmigrations of neutrophils by IL-8 and eosinophils by a combination of IL-8 and neutrophils were simultaneously examined, the capacity of eosinophils to migrate was significantly correlated with the number of neutrophils that migrate (P = 0.002, r = 0.54, n = 6). The time-course profile of TBM of eosinophils traced that of neutrophils: the TBM of neutrophils reached a plateau within the first 15 min, whereas eosinophil TBM mainly occurs 15–60 min after the initiation of reaction (n = 6, data not shown). In selected experiments, where the effect of IL-8 and neutrophils on the TBM of eosinophils was examined using both eosinophils and neutrophils from donors with mild asthma provided similar results: only a combination of IL-8 and neutrophils induced the TBM of eosinophils (n = 3, data not shown). Furthermore, when eosinophils were co-incubated with neutrophils from different donors, a similar phenomenon was observed: only a combination of IL-8 and neutrophils, but not IL-8 alone or neutrophils alone, induced the TBM of eosinophils (n = 3, data not shown). GRO-α (10 nM), another CXC chemokine, showed similar results: the TBM of

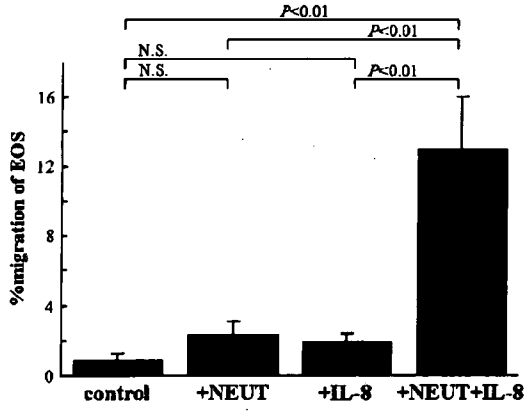

Figure 1. Effects of neutrophils and IL-8 (10 nM) on the TBM of eosinophils. The means ± SEM of 10 experiments using cells from different donors are shown. N.S., not significant.

eosinophils was significantly induced only when eosinophils were coincubated with neutrophils and stimulated with GRO-α (migrated eosinophils: 0.6 ± 0.3 by medium control, 1.2 ± 0.4 by a coincubation with neutrophils, P = n.s.; 0.8 ± 0.7 by GRO-α alone, P = n.s.; 7.1 ± 2.3 by a combination of GRO-α and coincubation with neutrophils, $P < 0.05$ versus the other three conditions, $n = 4$; Figure 2A). LTB_4 (100nM), which is chemotactic for both eosinophils and neutrophils, directly induced the TBM of eosinophils; however, the TBM of eosinophils was enhanced when both eosinophils and neutrophils were coincubated (migrated eosinophils: 1.0 ± 0.8 by medium control, 1.2 ± 0.9 by a coincubation with neutrophils, P = n.s.; 12.9 ± 4.6 by LTB_4 alone, $P < 0.05$ versus control; 23.6 ± 6.0 by a combination of LTB_4 and coincubation with neutrophils, $P < 0.05$ versus the other three conditions, $n = 5$; Figure 2B). Finally, eotaxin (3 nM), a CC chemokine that selectively stimulates chemotactic response of eosinophils, induced the TBM of eosinophils (migrated eosinophils: 2.9 ± 0.7 by medium control versus 59.5 ± 3.8 by eotaxin alone, $P < 0.01$). Coincubation with neutrophils did not modify the TBM of eosinophils in response to eotaxin (migrated eosinophils: 62.3 ± 4.5, P = n.s. versus eotaxin alone, $n = 5$; Figure 2C). Similar results were obtained when RANTES, another CC chemokine, was an activator ($n = 3$, data not shown).

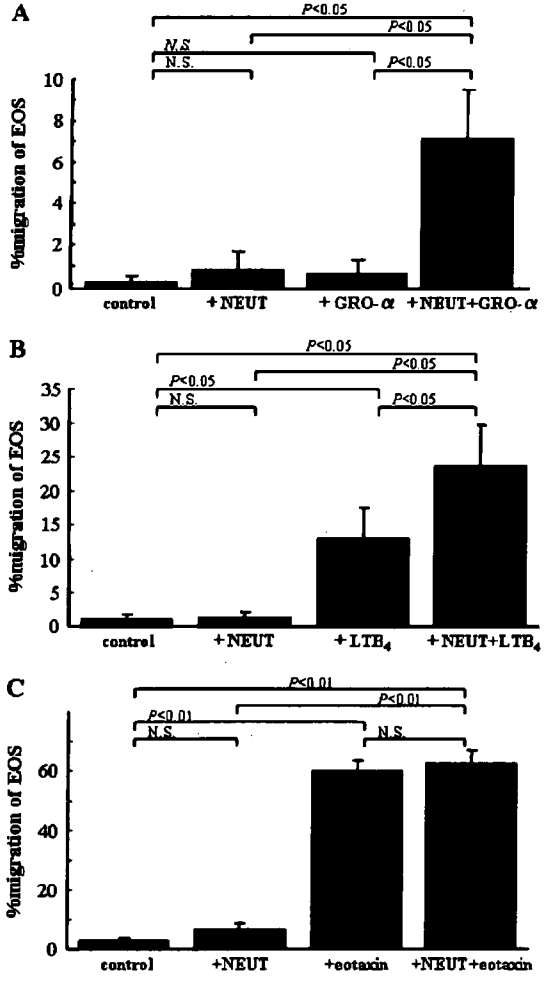

Figure 2. Effects of neutrophils and a variety of agonists on the TBM of eosinophils. Molecules used were GRO-α (10 nM, *A*), LTB_4 (100 nM, *B*), and eotaxin (10 nM, C). The means ± SEM of four to five experiments using cells from different donors are shown. N.S., not significant.

MMP-9, LTB_4, PAF, and TNF-α Are Involved in the Augmentation of Eosinophil TBM by IL-8–Stimulated Neutrophils

The results shown the above sections suggest that neutrophils act as regulators to affect TBM of eosinophils. Suppression of neutrophil-derived protease may lead to the suppression of TBM of eosinophils. To test this hypothesis, we inhibited MMPs, which work when cells digest the basement membrane during intrusion. An MMP-9 inhibitor (10 μM) could inhibit the augmented TBM of eosinophils in the presence of IL-8–activated neutrophils (Figure 3A). Similar results were observed when GM1489, an inhibitor of MMPs, was tested ($n = 5$, data not shown).

Activated neutrophils may secrete stimulatory molecules for eosinophils and thus augment their TBM as observed above. LTB_4, PAF, and TNF-α are the representative molecules secreted by neutrophils and are capable of activating eosinophils. To investigate whether they are involved, we inhibited the activity of these molecules and observed whether the TBM of eosinophils was suppressed. Reagents used were BIIL260, an LTB_4 receptor antagonist; WEB2086, a PAF receptor antagonist; and an anti–TNF-α monoclonal antibody (anti–TNF-α mAb, clone Mab11, mouse IgG1, 3 μg/ml). All of these reagents partially suppressed the TBM of eosinophils in the presence of IL-8–activated neutrophils but showed no effect in the absence (Figures 3B–3D). Similar results

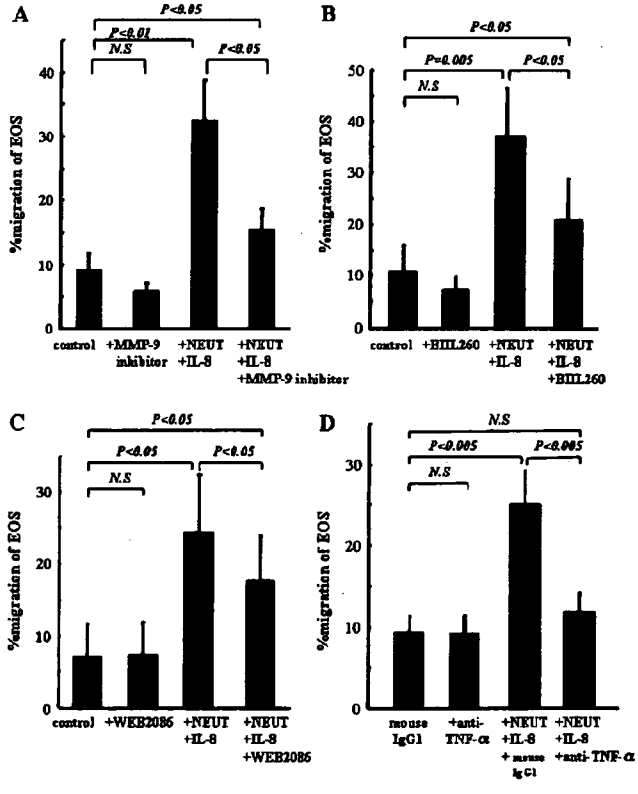

Figure 3. Effects of MMP-9 inhibitor (10 μM, *A*); BIIL260, an LTB_4-antagonist (1 μM, *B*); WEB2086, a PAF-antagonist (10 μM, C); and an anti–TNF-α antibody (clone Mab11, isotype mouse IgG1, 3 μg/ml; *D*) on the TBM of eosinophils in the presence of neutrophils stimulated by IL-8. The means ± SEM of five to seven experiments using cells from different donors are shown.